

# **Mechanically interlocked materials. Rotaxanes and catenanes beyond the small-molecule**

Sofía Mena-Hernando and Emilio M. Pérez

This is the accepted version of the following article: S. Mena-Hernando and E. M. Pérez, *Chem. Soc. Rev.*, 2019, 48, 5016, which has been published in final form at <https://doi.org/10.1039/C8CS00888D>.

## **To cite this version**

S. Mena-Hernando and E. M. Pérez, Mechanically interlocked materials. Rotaxanes and catenanes beyond the small-molecule. *Chem. Soc. Rev.*, 2019, 48, 5016, <https://repositorio.imdeananociencia.org/handle/20.500.12614/1733>

## **Licensing**

See RSC Terms & Conditions <https://www.rsc.org/journals-books-databases/librarians-information/products-prices/licensing-terms-and-conditions/>

## **Embargo**

This version (post-print or accepted manuscript) of the article has an embargo lifting on 16.08.2020.

# Mechanically interlocked materials. Rotaxanes and catenanes beyond the small-molecule.

Cite this: DOI: 10.1039/x0xx00000x

Sofía Mena-Hernando<sup>a</sup> and Emilio M. Pérez<sup>a,\*</sup>

Received 00th January 2012,

Accepted 00th January 2012

DOI: 10.1039/x0xx00000x

The mechanical bond presents a combination of the best features of covalent and supramolecular chemistries (stability and structural integrity), plus a unique dynamic nature, that make it a very interesting tool for materials chemistry. Here, we overview the chemistry of the mechanical bond applied to polymers, metal-organic frameworks (MOFs) and carbon nanotubes. We first describe synthetic strategies towards polycatenanes and polyrotaxanes, and highlight their potential impact in polymer chemistry, exemplified by their use to make stimuli-responsive gels and as binders in battery electrodes. We continue by showing how to include mechanically interlocked components in MOFs, and analyse the distinctive dynamic properties of the final constructs. Finally, we describe the strategies towards mechanically interlocked derivatives of single-walled carbon nanotubes (SWNTs), and discuss the potential of the mechanical bond to tackle some of the classic problems of SWNT chemistry.

## Introduction

The interest in molecules with non-trivial topology started as soon as medium sized molecular rings became synthetically viable, apparently as early as 1912.<sup>1,2</sup> Experimentally, the mechanical bond was born decades later, in the 60s,<sup>3</sup> with the seminal examples of the syntheses of catenanes (by Wasserman<sup>4</sup> and Schill<sup>5</sup>) and rotaxanes (by Harrison and Harrison<sup>6</sup>). However, the chemistry of mechanically interlocked molecules did not come of age until Sauvage pioneered the synthesis of interlocked molecules using templating methods.<sup>7,8</sup> Mechanically interlocked molecules (MIMs) are composed of multiple molecular fragments that are linked together as a consequence of their topology, so that separating them requires the breaking of the covalent structure of at least one of the constituents. The archetypal examples of MIMs are rotaxanes, in which one or more macrocycles are trapped onto a linear component (thread) by bulky substituents at its ends (stoppers) that prevent dissociation, and catenanes, where two or more macrocycles are interlocked as links in a chain. Whereas catenanes are clearly MIMs, this is not the case for rotaxanes in which the distinction between interlocked species (rotaxanes) and supramolecular complexes (pseudorotaxanes) can be much more blurred.<sup>9,10</sup> We have previously argued in favour of taking the structural integrity of the submolecular components after disassembly as a clear-cut criterion to discriminate between rotaxanes (MIMs) and pseudorotaxanes (supramolecular complexes). In this way, rotaxanes would disassemble to yield structures with different covalent connectivity than their original components (i.e. after the breaking of at least one covalent bond). On the other hand, pseudorotaxanes would

be rotaxane-like species in which disassembly to yield their intact components is feasible, even if under extreme conditions. This condition derives from the direct translation to chemistry of the mathematical norm, which states that objects that can be transformed into each other through continuous deformations, for instance, stretching and bending (i.e. really high temperatures), without tearing (i.e. breaking bonds) or gluing (i.e. making bonds), are topologically identical.<sup>11,12</sup> In this way, the mechanical bond is a unique tool that can be used to connect two covalent entities very intimately, with stability equal to their weakest covalent bond, *but* without modifying their structure. This exceptional characteristic make the mechanical bond an ideal candidate for tasks that cannot be carried out by either covalent or supramolecular chemistry, like the protection of unstable polyynes, cumulenes or dyes.<sup>13-18</sup> Moreover, the mechanical bond is inherently dynamic, that is, it allows one component to move with respect to the other along (or around) distances significantly larger than atomic vibrations. This latter characteristic has been exploited to synthesize molecular machinery based on MIMs, a fascinating field that has recently been recognized with the Nobel Prize in Chemistry 2016 to two MIM pioneers, Jean-Pierre Sauvage<sup>19</sup> and Sir J. Fraser Stoddart,<sup>20</sup> together with the most notable non-MIM molecular machinist, Ben L. Feringa.<sup>21</sup> The vast majority of the chemistry of MIMs has been developed on small-molecule fragments, and mainly in the frame of making artificial molecular machinery; consequently, plenty authoritative publications on the subject are available.<sup>22-38</sup> In the present review, we focus on the chemistry of the mechanical bond applied to materials chemistry, including polymers, metal-organic frameworks (MOFs), and carbon nanotubes. Indeed, the very

same characteristics of the mechanical bond that have made it very appealing for small-molecule chemistry (stability with structural integrity and dynamics) make it even more interesting a tool for materials science.

## Polymeric Materials Containing Mechanical Bonds

Compared to low molecular weight MIMs, mechanically interlocked polymers (MIPs), such as polyrotaxanes and polycatenanes, have aroused interest within the field of materials science as a consequence of the potential advantages of the dynamic nature of the mechanical bond -low energy barrier for the rotation of the rings, or the sliding of the rings along the polymeric thread- for the mechanical properties of the polymer. Comprehensive reviews by Gibson,<sup>39-41</sup> Stoddart,<sup>42</sup> Harada,<sup>43, 44</sup> and Takata<sup>45</sup> have already been published about these types of materials, so herein we will focus on the main general considerations and a selected number of recent examples.

### Polycatenanes

Poly[n]catenanes are polymers chains formed by interlocked rings, where [n] indicates the number of rings which are consecutively interlocked into a long chain without being interrupted by a covalent spacer in the polymer. Thus, poly[n]catenanes contain a very high concentration of topological bonds which confers a large number of degrees of freedom and mobility about the catenane moieties (Fig. 1a).

As a consequence of the high concentration of these topological bonds, it is expected that poly[n]catenanes have high strength and flexibility since they can present different chain conformations in the backbone repeat unit of the main chain, such as rotation, elongation, and rocking motions, compared to covalently connected molecules (Fig. 1a).<sup>1,3, 4, 40, 42, 45</sup>

Theoretical studies have been performed indicating that poly[n]catenanes with such mobility elements could exhibit a large loss modulus and a low activation energy for flow, as well as potentially acting as energy damping materials and/or elastomers with excellent toughness and mechanical properties controlled by an external stimulus.<sup>46-48</sup>

Depending on the location and connection of the catenane subunit, different types of polycatenanes can be found, such as, main chain polycatenanes, side chain polycatenanes, polycatenanes prepared by cyclization of polyrotaxanes, or polycatenane networks (Fig. 1).

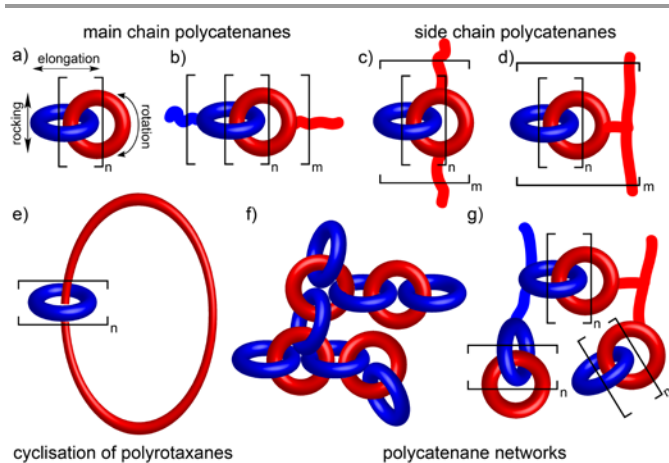


**Fig. 1** Main types of polycatenanes: a) linear polycatenanes, in which the polymer backbone is exclusively formed of interlocked rings, or b) where the catenanes are incorporated into the polymer backbone. From c) to d) side chain polycatenanes, polycatenanes based on cyclic polymers and, polycatenanes networks. The types of large-amplitude internal motions in such structures are depicted in a).

The pioneering works related with the synthesis of polycatenanes were focused on oligocatenanes such as poly[2]catenanes in which [2]catenane moieties are incorporated into the backbone of conventional polymers<sup>46, 49-56</sup> (Fig. 1d), polymeric [2]catenanes (two interlocked cyclic polymers, Fig. 1e)<sup>57</sup> and, poly/oligocatenanes with unclearly-defined architectures (Fig. 1f and g).<sup>58, 21</sup>

Linear poly[n]catenanes (Fig. 1a), which do not have covalent bonds in their backbone structure, are particularly attractive, since the potential benefits of the topologically bonded structures are maximised. However, the synthesis of such linear poly[n]catenanes has been one of the greatest challenges for synthetic and polymer chemists for decades, because the ring-closing reaction step generally occurs with low efficiency.

Since the discovery of metallocatenanes by Dietrich-Bucheker and Sauvage in 1983<sup>8</sup> different oligocatenanes have been synthesized, in the pathway towards true poly[n]catenanes. A classic example of an oligocatenane, composed of five macrocyclic units, was synthesized by Amabilino and Stoddart in 1994 and became known as “olympiadane” due to its similarity to the five interlocked rings in the symbol of the Olympic Games (Fig. 2a).<sup>59</sup> Recently, Iwamoto and coworkers achieved the synthesis of other [5]catenanes, through the dimerization of [2]catenane-containing rotaxanes.<sup>60</sup> With the maximum degree of polycatenation at the time between 1 and 5, in 1997 Stoddart and coworkers were able to use a stepwise approach to prepare an impressively complex branched [7]catenane (Fig. 2b).<sup>61</sup>

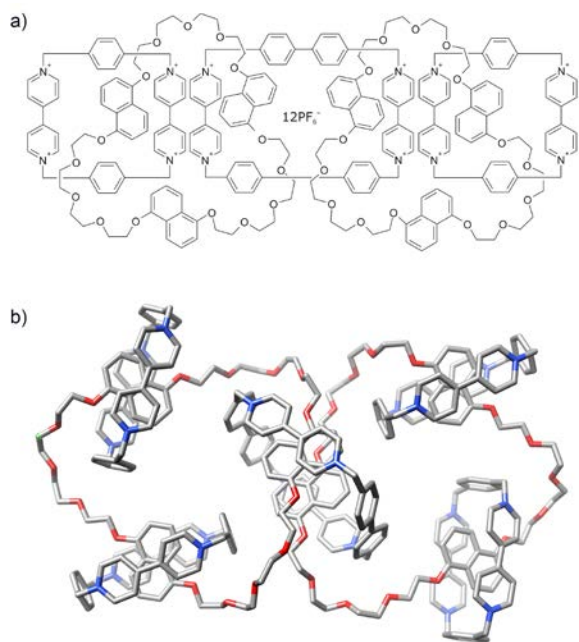


**Fig. 2** a) Chemical structure of olympiadane<sup>59</sup> and b) solid-state structure of the [7]catenane reported by Stoddart and co-workers.<sup>61</sup>

The research towards obtaining poly[n]catenanes formed by more than 7 interlocked rings has continued since then. In 2015, Meijer, Di Stefano and their coworkers, synthesized oligo[n]catenanes with at least 7 interlocked rings by ring opening polymerization of metalla[2]catenanes, although the structure of these oligo[n]catenanes was not clearly defined.<sup>58</sup>

Despite these considerably good results, it is well known that the step-wise strategies are not efficient methodologies to obtain long-chain poly[n]catenanes. An interesting solution to this challenge was proposed by Takata, Kihara and co-workers in 2004, consisting of converting a bridged poly[2]catenane into poly[n]catenanes by using 1,2 dithiane as monomer.<sup>52</sup>

However, no examples of poly[n]catenanes synthesized through this methodology have yet been reported in the literature.

Only very recently, Rowan and co-workers have successfully prepared poly[7-27]catenanes, branched poly[13-130]catenanes, and cyclic poly[4-7]catenanes via metallosupramolecular polymers templating strategies, followed by an efficient ring closing reaction and demetallation of the resulting metallated poly[n]catenane (Fig. 3a).<sup>62</sup> This synthetic strategy was performed by using the terdentate ligand 2,6-bis(N-alkyl-benzimidazolyl) pyridine (Bip, Fig. 3b), which binds transition metal ions such as Zn<sup>2+</sup> or Fe<sup>2+</sup>. In this fashion Rowan's group designed the 68 membered ditopic Bip macrocycle **2** with the threading molecule **1** followed by a subsequent ring closing reaction of **1**.

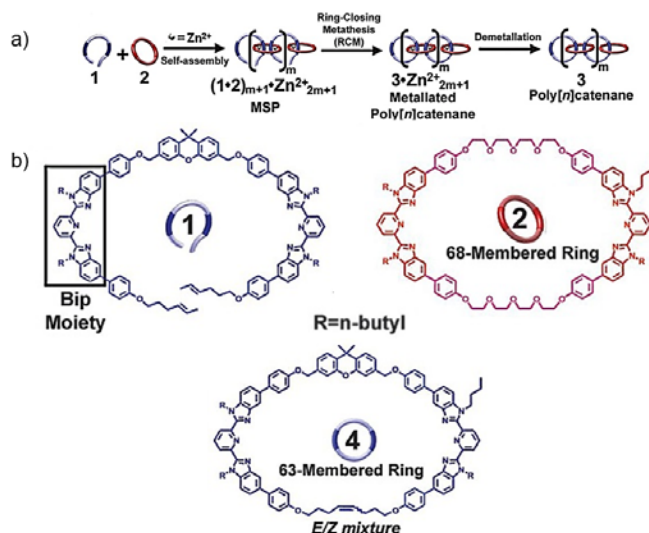


**Fig. 3** Rowan and co-workers' strategy to synthesize poly[n]catenanes a) synthesis of poly[n]catenanes **3** via assembling **1** and **2** into a metallo-supramolecular polymer (MSP) followed by ring-closing to yield poly[n]catenane and demetallation; and b) the structure of **1**, **2** and **4** (ring-closed product of **1**). Adapted from Wu et al. *Science*, 2017, **358**, 1434-1439. Reprinted with permission from AAAS, copyright 2017.

Considering the principle of maximal site occupancy, in which two Bip units in a macrocycle cannot bind the same Zn<sup>2+</sup> ion is expected that each Bip unit in **2** must form a 2:1 Bip:Zn<sup>2+</sup> complex with a Bip unit in **1**, maximizing the enthalpy factor. The large binding constant between Bip and Zn<sup>2+</sup> ensures an efficient ring closing metathesis (Fig. 3a). The demetallation process was performed using tetrabutylammonium hydroxide and the noninterlocked by-products were removed through demetallation-remetallation processes, since metal ions interact preferentially with interlocked ligands because the entropic cost is significantly less than the interaction with noninterlocked free ligands. This new methodology represents a conceptual breakthrough, as similar design principles can be applied to different ligand-metal pairs, so it is in principle expected that more poly[n]catenanes will be developed in the very near future.

### Polyrotaxanes

Polyrotaxanes (PR) are polymers formed by (or that contain) rotaxane units repetitively. For the same reasons described for polycatenanes, that is, the potential benefit arising from the large-amplitude motions allowed in mechanically linked components (Fig. 4a), PRs have aroused interest in the field of polymer chemistry. We can find main chain polyrotaxanes in which the main chain is either connected through covalent bonds (a linear polymer as thread, Fig. 4a or several rotaxanes connected covalently through their macrocycles as shown in Fig. 4b), or through their stoppers<sup>63</sup>), through host-guest interactions (a supramolecular PR, Fig. 4d) or itself mechanically interlocked, as in daisy chains (Fig. 4e); and side chain PRs consisting a polymer backbone branched with multiple rotaxane architectures (Fig. 4c).<sup>42, 43, 44, 45</sup>

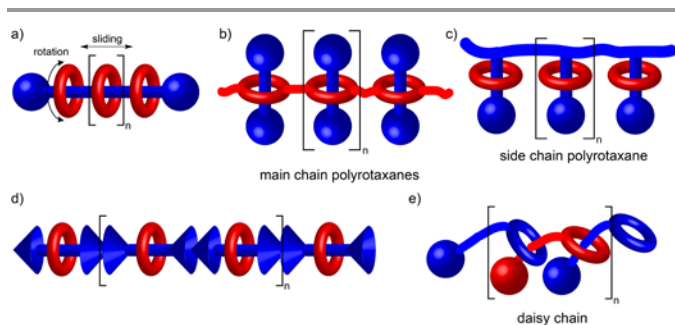


**Fig. 4** Main types of polyrotaxanes. a, b, d and e) main chain polyrotaxanes, in which the polymer backbone is connected covalently (a and b), supramolecularly (d) or mechanically (e); and side chain-polyrotaxanes (c), in which rotaxane units branch out of the polymer backbone. The main types of large-amplitude internal motions in polyrotaxanes are depicted in a).

Synthetically more accessible than polycatenanes, many kinds of PRs have been synthesized. In fact, the very first rotaxane was also the first side-chain polyrotaxane as it was synthesized by threading a macrocycle attached to a polymer resin.<sup>6</sup> Since then, many different combinations of polymer chains and macrocycles (crown ethers, cyclophanes, cucurbiturils, cyclodextrins...) have been used to synthesized PRs.<sup>44,64-67</sup>

As expected, these structures show distinct properties compared to noninterlocked mixtures of the components. Perhaps one of the most impressive examples to date are the different types of PR gels that can be found in the literature. Polymer hydrogels are often classified following the type of crosslink points. In this way, we can distinguish two classes: the covalent hydrogels, with permanent crosslinks (chemical bonding), and the physical hydrogels which are obtained by non-covalent interactions such as ionic or hydrogen bonding (physical bonding) that act as reversible crosslinks.

The idea of implementing PRs in polymeric gels was to the best of our knowledge first postulated by de Gennes in 1999.<sup>68</sup> In this new class of PR-containing supramolecular networks, the crosslink points are not fixed but sliding. Such materials were, accordingly, called slide-ring or topological gels and were first described experimentally by Okumura and Ito in 2001.<sup>69</sup> The sliding network architecture was achieved by the use of PRs, whose chemical structures were based on cyclodextrin macrocycles (CDs) and poly(ethylene glycol).<sup>69-72</sup> In later studies, other polymers such as poly(dimethylsiloxane) and poly(N-isopropylacrylamide), were used as well.<sup>73,74</sup> After this discovery, many examples of such topological polymer networks have been published and applied in different fields, such as photoresponsive gels<sup>75</sup>, chromic gels<sup>76</sup> and even as anti-scratch coatings for cell phones.<sup>77</sup>

The presence of PRs (cross-linked or freely moving) has an impact on dynamic and physical properties of the material, such as viscosity,<sup>78</sup> extensibility<sup>79</sup> and mechanical strength.<sup>77</sup> The crosslinking points in PR gels influence the mechanical behaviour differently than the entanglement of polymer chains or the fixed junctions in chemical gels and rubber. In fact, PR gels show quite low Young's modulus compared to chemical gels with the same crosslinking density. Moreover, Sawada and co-workers have demonstrated that rotaxane crosslinking polymers have

higher fracture stress and strain than those of covalently cross-linked polymers, thanks to the increased network homogeneity by the rotaxane cross-links.<sup>80, 81</sup>

As a consequence of topological restrictions, the polymer chain in PR gels can slide through the crosslink but cannot be released from it totally. This allows the conformational relaxation of the polymer along its chain's axis, called pulley effect.<sup>77</sup> In addition to this, free (uncrosslinked) rings that remain in the PR structure lead to a heterogeneous density distribution, which allows a transfer of the polymer's conformational entropy to the free cyclic molecules, resulting in a substantial entropy loss for the polymer. This is in strong contrast to conventional polymeric materials (gels and rubbers), which do not have such entropy, and has a considerable impact on their elasticities and Young's moduli (Fig. 5). These materials have finite equilibrium moduli, which arise from the entropic elasticity of the polymer conformation between fixed crosslinks.

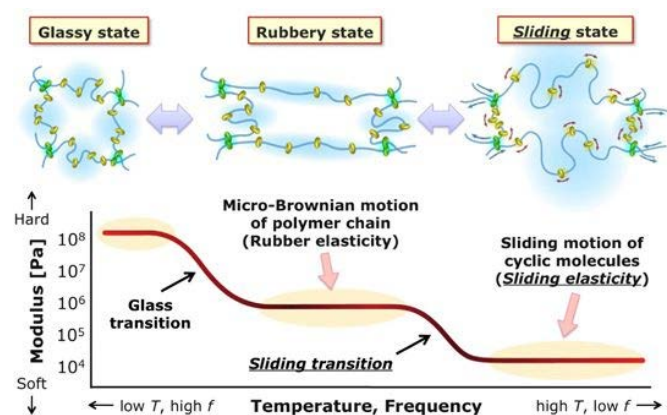


**Fig. 5** Mechanical dynamics of polyrotaxane materials: besides the typical a glass transition between glass and rubber states of covalent polymers, polyrotaxane materials shows a sliding transition and sliding state. Reprinted by permission from Springer Nature, Polymer Journal, copyright 2011.<sup>77</sup>

Ito and co-workers have studied viscoelasticity in PRs, which describes how, depending on the molecular dynamic properties, a polymer material can behave as a viscous fluid or as elastic solid. Further, using NMR and neutron spin echo spectroscopy, they showed that PR gels exhibit different viscoelastic relaxation dynamics depending on the size of the ring component. Gels with larger rings showed relaxation times up to 5 times slower than those with smaller rings. Nevertheless, gels with differently sized rings exhibited a common relaxation mechanism of chain sliding along the distance between crosslinks. These results indicate that the chain sliding motion through the larger ring cavity was significantly slower. The decelerated chain sliding was attributed to an increase in the interactions between the chain and the inner surface of the larger rings. This implies that the interactions can be mediated by solvent molecules interpenetrated in the extra cavity of the larger rings. Thus, this study suggests a possible method for controlling the dynamics of PR materials by designing molecular interactions based on host-guest chemistry.<sup>82</sup> In contrast with the soft materials, where the CD rings are able to slide along the polymer chain, this motion is strongly inhibited in solid materials after the glass transition. Meanwhile, the

threading polymer retains a considerable mobility within this frozen CD ring framework, allowing strong secondary relaxations. Such secondary relaxations are further enhanced by a remarkably high degree of rotational motion of the polymer in the frozen CD ring framework. Both these molecular relaxation motions are related to the solid properties, strongly affecting the strength of the polymer glass. The most characteristic example is a class of ductile glasses prepared via melt-press molding of a thermoplastic PR.<sup>83,84, 85</sup> It is worth to mention that the process of melt-press molding itself allows the creation of different PR glasses from one polymer. To do so, the thermal fluctuations during the glassy transition can be exploited to trigger more profound stress-induced structural changes, potentially leading to the development of novel hard yet flexible materials.

Recently, the influence of the position of the rings within a PR glass was investigated.<sup>86</sup> The study was conducted using a triblock copolymer Poly(ethylene oxide)-*b*-poly(propylene oxide)-*b*-poly(ethylene oxide) (PEO-PPO-PEO) threaded through  $\beta$ -CD rings that can be chemically modified to bear hydrophilic or hydrophobic groups (Fig. 6a). When bearing the hydrophilic groups, the CDs prefer to locate in the central section of the polymer thread, forming a free-encapsulated-free structure, that can be compared to an ABA-type copolymer. This tendency can be reversed by silylation, which makes the CDs hydrophobic and changes their preference to the end sections of the thread, forming an encapsulated-free-encapsulated sequence, or BAB stacking (Fig. 6b and c). Therefore, the molecular manipulations bring about a conformational change through sub-molecular motion, which in turn provokes a change in the intermolecular self-assembly preferences, which is finally reflected in a drastic change in the mechanical properties from a melt state to an elastic behaviour (Fig. 6 d and e).

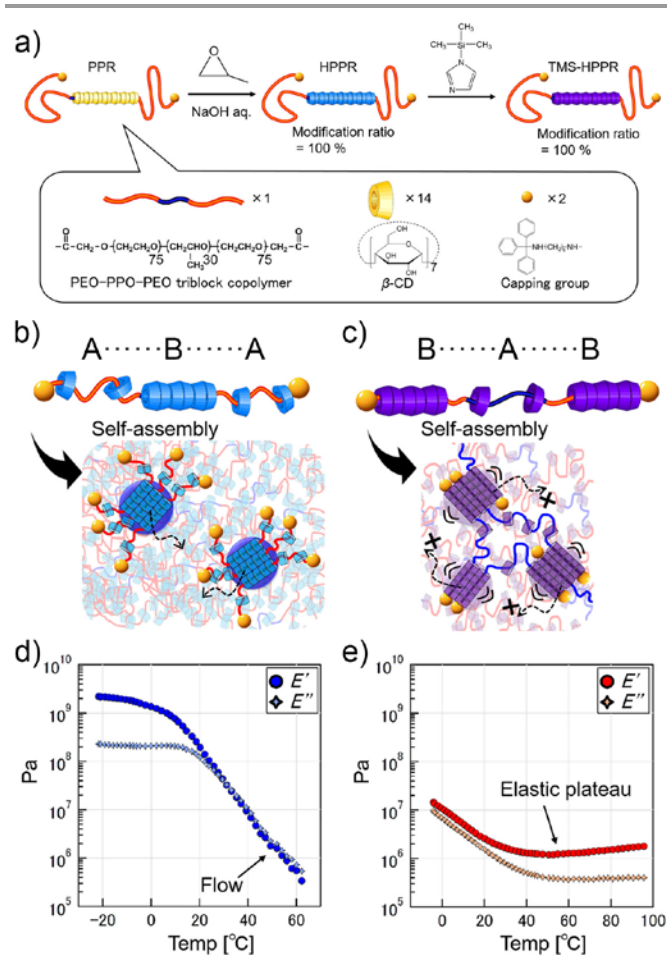


**Fig. 6** a) Chemical structures and synthetic scheme of PEO-PPO-PEO-CD polyrotaxanes (PPR), bearing hydrophilic hydroxypropyl groups (HPPR) and hydrophobic trimethyl silyl groups (TMS-HPPR). b and c) Results of dynamic mechanical analysis and the schematic illustrations of (b) HPPR and (c) TMS-HPPR above the  $T_g$ . Adapted from S. Uenuma, R. Maeda, K. Kato, K. Mayumi, H. Yokoyama and K. Ito, *ACS Macro Letters*, 2019, 8, 140-144, 2019 with permission from the American Chemical Society, copyright 2019.

Other kinds of glassy PRs based on CDs have also been synthesized. Taneda et al. have prepared a PR structure composed of PEO and  $\alpha$ -CD at the outermost surface of a glassy poly (methyl methacrylate) film. The dynamics of the PEO chain at the water interface can be modulated by threading the CD molecules on PEO. With this strategy, biological responses (such as protein adsorption and platelet adhesion) can be modified depending on the degree of complexation of polymer chains with the CD rings.<sup>87</sup>

Takata and co-workers synthesized crosslinked PRs from vinyl polymers, and both CD<sup>88</sup> and crown ether macrocycles.<sup>89-91</sup> The authors observed, similar to other studies, a macrocyclic effect that leads to polymers with higher swellability, enabled by the high mobility of the wheel through the polymer chains.

Another strategy towards dynamic materials consists in the use of inclusion complexes formed by CD rings (host) and non-covalent crosslinks (guest). Such soft materials can form gels with dynamic properties, such as the self-healing ability, which is particularly desirable to increase the useful life of these materials.

Most conventional polymers lack the self-healing ability, as the covalent bonds do not typically allow dynamic re-organization of the polymer structure upon stress, with the exception purposely designed polymers including dynamic covalent bonds that can be reversibly formed and broken in response to adequate stimuli.<sup>92-96</sup>

The intrinsically dynamic nature of non-covalent interactions allows the self-healing of properly designed polymers. Two surfaces of such can be brought into contact, upon which the free host and guest units on the surface form the same host-guest bond that constitutes the bulk, thus recovering the initial bulk stress strength. This strategy of formation of complementary complexes and the polymerization of inclusion complexes in aqueous solutions is widely being used to create self-healing polymers.<sup>97-99</sup>

Along these lines, Nakahata and co-workers have reported a supramolecular hydrogel consisting of high molecular weight poly (acrylic acid) (pAA) with ferrocene (Fc) and  $\beta$ -CD moieties. The self-healing properties, such as re-adhesion between cut surfaces, can be controlled using redox reactions inducing a sol-gel phase transition in the supramolecular hydrogel (Fig. 7a).<sup>100</sup> The study was performed using NaClO (aq. 14 mM) as an oxidant and glutathione (GSH) as a reductant. Under oxidizing conditions, the viscosity of the gel decreases transforming the hydrogel into the sol. In contrast, under reducing conditions the sol state recover elasticity reverting it back to the hydrogel (Fig. 7b). This behaviour is due to the larger affinity of  $\beta$ -CD towards the hydrophobic neutral reduced state of the Fc compared to the hydrophilic cationic oxidized state,  $\text{Fc}^+$ . The same switching behaviour can be obtained by electrochemical stimulation. The hydrogel decreases in elasticity under electrochemical oxidation, and consequently is transformed into the sol. The reduction was carried out by heating the sol at 50°C, which recovered the typical elasticity of the hydrogel (Fig. 7c).

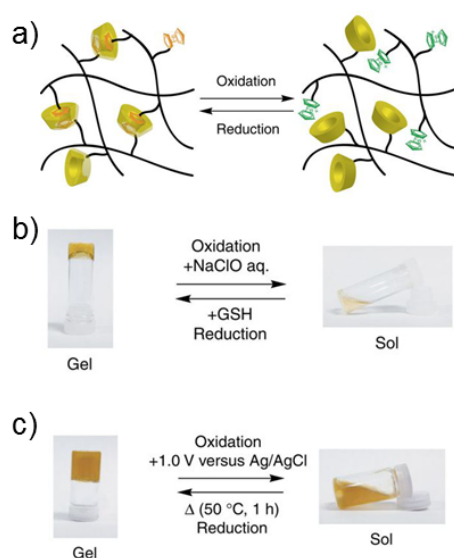


**Fig. 7** a) Schematic illustration of the redox-mediated sol-gel transition described by Nakahata and co-workers.<sup>100</sup> b) Sol-gel transition experiment using NaClO as oxidant to the pAA- $\beta$ -CD/pAA-Fc hydrogel induced a phase transition into the sol state, and continuous addition of glutathione (GSH) as reducing agent to the sol

recovered the elasticity to yield the hydrogel again. c) Sol-gel transition experiment using electrochemical reactions. Adapted from Nakahata et al. *Nat. Comm.*, 2011, **2** (511), 1-6. Reprinted by permission from Springer Nature, copyright 2011.

In 2016, Harada's group reported self-healing materials based on PRs and vinyl polymers cross-linked by covalent reversible bonds. In particular, they have prepared gels by using 4-vinylphenylboronic acid (PB) and acrylamide (AAm) cross-linked with boronate linkages in presence of hydroxypropylated PR (HPPR) and hydroxypropylated pullulan (HPPul) (Fig. 8). Unlike conventional polymers, the mobility of the ring molecules along the axle in the polyrotaxane and the sliding nature of the cross-linker are proven to provide both "physical" and "chemical" self-healing properties on the resultant materials. PR-PB gel exhibit ~100% healing, whereas the Pul-PB gel showed only ~20% healing. Therefore, the PR structure inside of the gel plays an important role in performing an efficient self-healing effect extending the lifespan of the material.<sup>101</sup>

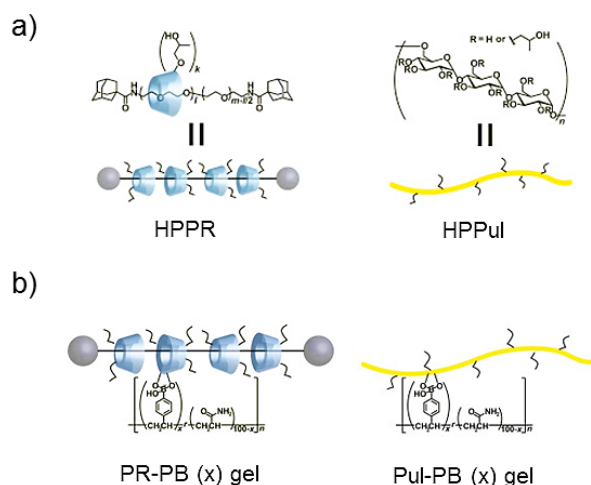


**Fig. 8** Chemical structure of the gels. a) Schematic representation of HPPR and HPPul. b) Chemical structures of the PR-PB (x) gel and Pul-PB (x) gel. X, represents the mol % content of cross-linker units (PB) in the vinyl polymerization. Adapted from M. Nakahata, S. Mori, Y. Takashima, H. Yamaguchi and A. Harada, *Chem*, 2016, **1**, 766-775, with permission from Elsevier, copyright 2016.

Stimuli-responsive PR are particularly interesting. Harada and co-workers designed a photoresponsive supramolecular actuator by integrating host-guest interactions and photoswitching ability in a hydrogel.<sup>102</sup> A photoresponsive supramolecular hydrogel with  $\alpha$ -CD as a host molecule and an azobenzene derivative as a photoresponsive guest molecule exhibits reversible macroscopic deformations in the same way that was previously reported by Zhao and Stoddart.<sup>103</sup> Azobenzene was selected as guest molecule because the association constant of  $\alpha$ -CD for *trans*-azobenzene ( $K_a = 12,000 \text{ M}^{-1}$ ) is larger than that for *cis*-azobenzene ( $K_a = 4.1 \text{ M}^{-1}$ ). Therefore, azobenzene affects the photoinduced deformation and remote controllability. Using water as solvent, the azobenzene moieties were isomerized from the *trans* to the *cis* conformation by irradiation with UV light (Fig. 9).

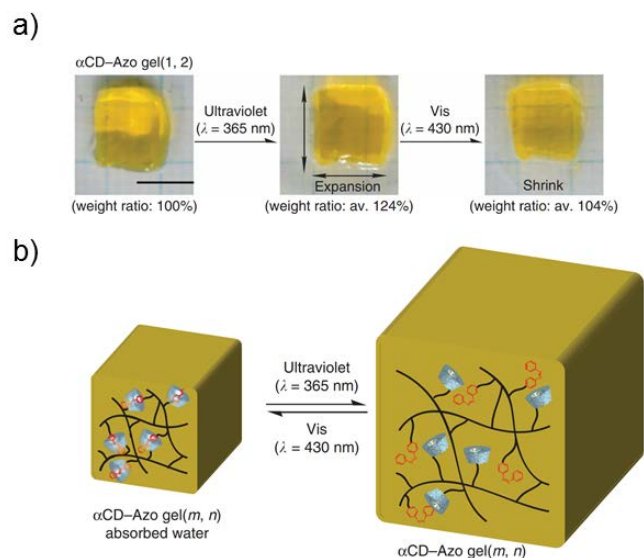


**Fig. 9** a) Photographs of the volume change of  $\alpha$ -CD-Azo gel irradiated by ultraviolet and Vis light. Scale bar, 5 mm; b) Schematic illustration of the expansion-contraction of  $\alpha$ -CD-Azo gel irradiated by ultraviolet and Vis light. After ultraviolet irradiation, which induces isomerization from the *trans*- to *cis*-form, the complex between  $\alpha$ -CD and Azo units decomposes to expand  $\alpha$ -CD-Azo gels. Vis irradiation causes isomerization from the *cis*- to *trans*-form, and complexation between  $\alpha$ -CD and the Azo units regenerates. Adapted from Y. Takashima, S. Hatanaka, M. Otsubo, M. Nakahata, T. Kakuta, A. Hashidzume, H. Yamaguchi and A. Harada, *Nat Commun*, 2012, **3**, 1270, reproduced in compliance with CC-BY-NC-SA License.

The photoisomerization caused the dissociation of inclusion complexes decreasing the crosslinking density of the material, leading to the swollen state of the gel. When the swollen state is irradiated with visible light, *cis*-azobenzene moieties were isomerized back to the *trans* form. Then, the crosslinking density became higher leading to the shrunk state. This molecular change leads to a deformation of the supramolecular hydrogel depending on the incident direction. If the gel is cut in a ribbon shape, suspended in water and irradiated with UV light, only a thin layer close to the surface of the irradiated side was swollen. This is because light can be only absorbed by the azobenzene molecules in close proximity to the surface. Due to this asymmetry, the ribbon-shaped gel bent to the direction opposite to light source.<sup>104, 105</sup>

Recently, one of the most interesting applications of PRs has focused on increasing the useful life of lithium (Li)-ion batteries.<sup>106</sup> Although the massive volume change of Si during repeated charge-discharge cycles has been identified as the main origin of insufficient cycle lives of Si anodes, it has recently been recognized that binders can contribute substantially to improve their cycle lives.<sup>107, 108</sup> Polyvinylidene difluoride (PVDF) polymer has frequently been used as binder but, is not appropriate for Si anodes because it exhibits weak van der Waals interactions with Si and the copper current collector.

The stress dissipation during the expansion of Si is the key to the operation of Si anodes. Coskun, Choi and co-workers have considered the use of pulleys which can help through a stress-release

mechanism.<sup>109</sup> They have developed a new binder for SiMP anodes consisting on PR comprising PEG threads and  $\alpha$ -CD rings functionalized with 2-hydroxypropyl moieties. Some of these moieties are covalently connected with polyacrylic acid (PAA) acting as pulleys as some rings are fixed along the polymer chain and, rings unfixed which can move freely (Fig. 10a). The movement of the pulleys reduce the tension exerted on the polymer network (Fig. 10b).

Additionally, these materials present different states. In their pristine state, the  $\alpha$ -CD rings are distributed randomly along the PEG thread. However, once the SiMPs are expanded during a lithiation process, the stretching of polyrotaxane and PAA chains leads to the movement of the ring components closer to each other to reduce mechanical stress. Subsequently, delithiation process takes place, making it possible for the rings to return from this high-energy state to their pristine state via entropic repulsion.<sup>77</sup>

Furthermore, in a battery cycle, the SiMPs are pulverized.<sup>110, 111</sup> PR keeps the pulverized Si particles coalesced, which is critical for preserving the electrode morphology. In contrast to this behaviour, in a simple linear PAA binder without PR, pulverized Si particles remain apart. As a consequence, patchy solid electrolyte interphase layers grow in the interparticle space (Fig. 10c). The continuous growth of these layers in prolonged cycles lead to an electrical disconnection between Si particles.<sup>109</sup> Therefore, PR-PAA-SiMP electrode exhibited a cycling performance better than a PAA-SiMP electrode. It has been observed how measuring at 0.2 C (0.64 mA cm<sup>-2</sup>), the PR-PAA-SiMP with an initial area capacity of 2.67 mAh·cm<sup>-2</sup> preserved 2.43 mAh·cm<sup>-2</sup> after 150 cycles, which corresponds to 91% of capacity retention. By contrast, under the same conditions the PAA-SiMP electrode starts to lose its capacity from the beginning and retained only 48% of the initial capacity after 50 cycles.



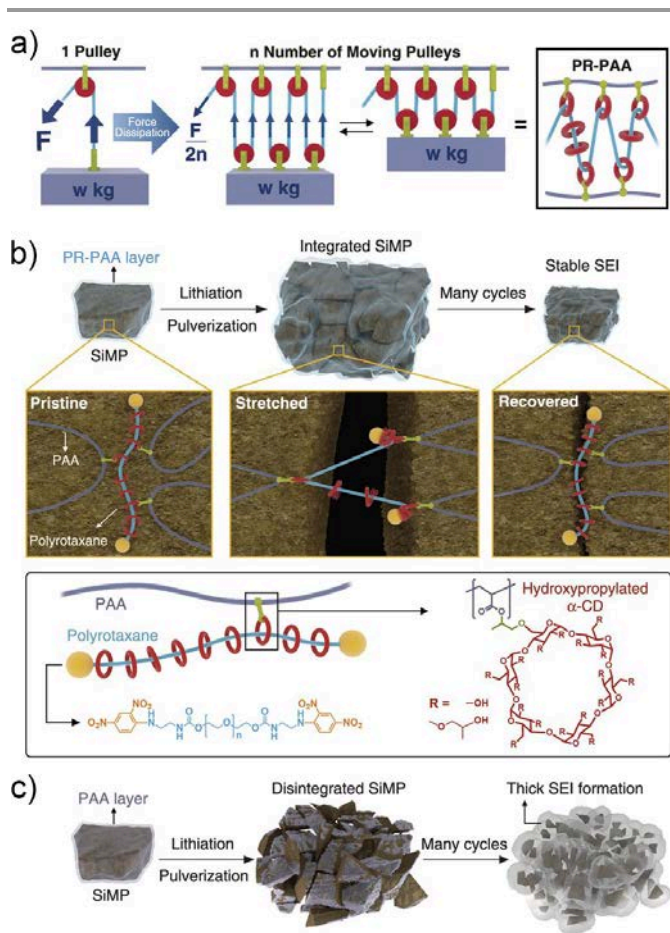


**Fig. 10** Stress dissipation mechanism of PR-PAA binder for SIMP anodes: a) The pulley principle to lower the force in lifting an object. b) Graphical representation of the operation of PR-PAA binder to dissipate the stress during repeated volume changes of SIMPs, together with chemical structures of polyrotaxane and PAA. c) Schematic illustration of the pulverization of the PAA-SIMP electrode during cycling and its consequent SEI layer growth. Adapted from Choi et al. *Science*, 2017, **357**, 279-283, with permission from AAAS, copyright 2017.

## Mechanical links in Metal-Organic Frameworks

Metal Organic Frameworks (MOFs) are three-dimensional materials, built up by inorganic species (metals or clusters) that are coordinated by organic ligands in a crystalline porous network.<sup>112-117</sup> These materials show high porosity and surface areas, which makes them appealing for applications related to catalysis,<sup>118-120</sup> gas storage,<sup>121, 122</sup> sensing,<sup>122, 124</sup> and drug delivery.<sup>123-129</sup> Although MOFs are extensive in number, the evolution of these materials through the addition of complexity to their structures remains an area of interest today, providing the key to enhanced functionality.

It is well known that molecules in solution operate through a random and incoherent motion. The term ‘robust dynamics’<sup>130</sup> has been coined to describe the dynamic properties presented by frameworks constituted by MIMs inside. The insertion of MIMs into the rigid architecture of MOFs contributes to include large-amplitude motions, such as rotation and translation, without al-

tering the hard and structural backbone of the material. This concept implies avoiding the uncontrolled movement of the molecules by confining them within a three-dimensional extended structure. These materials are named metal-organic rotaxane frameworks (MORFs, Fig 11.).<sup>131, 132</sup>

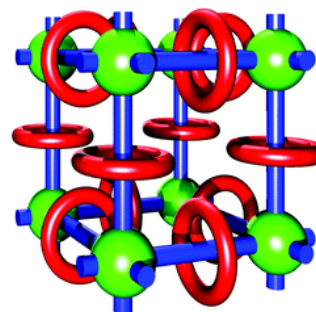


**Fig. 11** General structure of a metal-organic rotaxane framework (MORF). Reproduced from S. J. Loeb, *Chem. Commun.*, 2005, 1511-1518, with permission from The Royal Society of Chemistry, copyright 2005.

In 2000, Kim and co-workers reported the first 3D structure containing rotaxanes. The synthesis was performed from a diamino-alkane and a curcubituril ring through hydrothermal conditions with  $Tb(NO_3)_3$ .<sup>133</sup> Subsequently, in 2005 Loeb and Wisner published 3D structures based on a pyridine-N-oxide [2]pseudorotaxane with different lanthanide ions.<sup>134, 135</sup> Nevertheless, none of these structures displayed the dynamic motion expected from interlocked molecules.

In 2012, Loeb and co-workers prepared the first dynamic MORF named as UWDM-1 (University of Windsor Dynamic Material) with formula  $[Cu_2(MIM)(H_2O)_2] \cdot 3H_2O$  (Fig. 12). The MIM moiety consisted of an aniline-based axle, which can be protonated to form a benzyl-anilinium cation and interact with a crown ether macrocycle labelled with two deuterium atoms. The dynamic properties were studied by variable temperature (VT) and  $^2H$  solid-state (SS) NMR spectroscopy. The experiments demonstrated that the crown ether ring can undergo free rotation through the coordination polymer backbone.

The rotation of the wheel component in UWDM-1 is temperature-dependent and reversible. Solvent molecules can bind with the macrocycles through hydrogen bonding, leading to a static situation of the ring. However, when the structure is heated under vacuum at 150 °C, the solvent molecules are removed from the channel as well as from the copper centres, undergoing free rotation of the crown ether. In this way, the rotation can be activated/deactivated without affecting the rigid MOF architecture.<sup>136</sup>

On the other hand, the variation of the size of the macrocycle also affects the dynamic properties of the material. The rate of rotation depends on the size and shape of the macrocycle. The corresponding study was carried out by V.N. Vukotic et al, by varying the size of the crown ether macrocycles from [22] crown-6, [24] crown-6, [26] crown-6 to benzo [24] crown-6. The highest mobility was observed in UWDM-1 ([24] crown-6) which has three different motions: a two-site jump of  $CD_2$  groups, a partial rotation of the macrocyclic ring and full rapid

rotation of the ring. All three types of movements present a higher rate with increased temperature.<sup>137</sup>

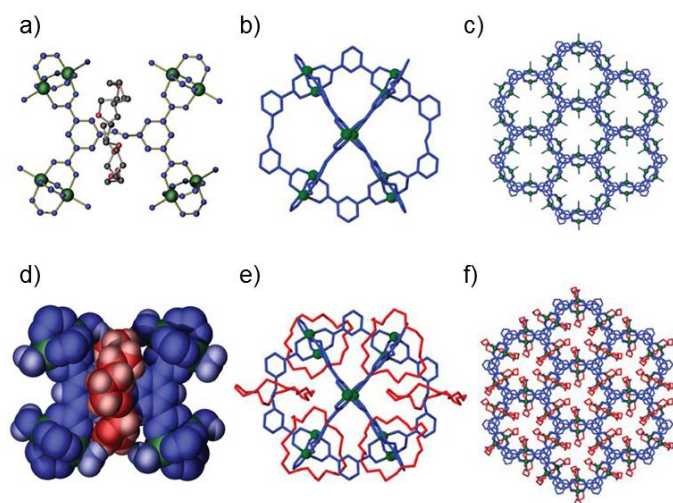


**Fig. 12** UWDM-1 structure determined by single crystal X-ray diffraction. A) Ball-and-stick representation of a single unit of the MIM coordinated to four Cu(II) paddlewheel clusters. B) space-filling model. C) Polyhedron comprising six paddlewheel units with macrocyclic rings omitted. D) As in c, but with macrocyclic rings shown. E) Linked polyhedra, with macrocyclic rings omitted, viewed down the c-axis, showing the channels that contain H<sub>2</sub>O. F) As in e, but with macrocyclic rings shown. Adapted from V. Nicholas Vukotic, Christopher A. O'Keefe, Kelong Zhu, Kristopher J. Harris, Christine To, Robert W. Schurko, and Stephen J. Loeb, *J. Am. Chem. Soc.*, 2015, **137**, 9643-9651 with permission from the American Chemical Society, copyright 2015.

Subsequently, Loeb and co-workers synthesized new dynamic MOFs, in which the dynamic motion of the macrocycle can be controlled by a reversible phase change in the framework of the material. Between UWDM-2 (1,4-diazophenyl-dicarboxylate) and UWDM-3 (1,4-biphenyl-dicarboxylate) only the UWDM-3 showed a gradual phase change over a temperature range of 100-125°C (Fig. 13).  $\beta$ -UWDM-3 phase is due to desolvation and deformation of the structure of the MOF. This phase change can be also promoted by solvent exchange with CH<sub>2</sub>Cl<sub>2</sub> and mild drying of the sample. Moreover, this phase change is reversible, as it can be reversed by re-exposure of the desolvated sample to DMF.<sup>138</sup>

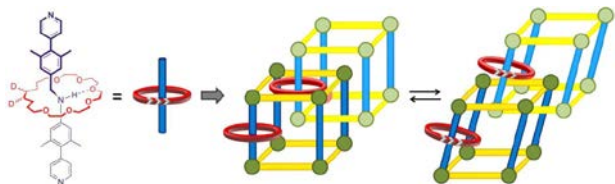


**Fig. 13** Schematic illustrating of the conversion between the  $\alpha$ -form (left) and desolvated  $\beta$ -form (right) of UWDM-3, which is accompanied by release of the macrocyclic wheel into a free volume space within the MOF allowing for the full range of dynamic motions as observed by <sup>2</sup>H SSNMR. Adapted from Kelong Zhu, V. Nicholas Vukotic, Christopher A. O'Keefe, Robert W. Schurko, and Stephen J. Loeb. *J. Am. Chem. Soc.*, 2014, **136**, 7403-7409, with permission from the American Chemical Society, copyright 2014.

One of the most characteristic ligands studied has been the H-shaped rigid axle with different crown ethers (Fig 14).<sup>139</sup> Baggi and Loeb have studied linkers which present a specific topology,

allowing to modulate the ability to dial-up different donor set for complexation to metal ions (such as Li<sup>+</sup>, Cu<sup>+</sup> and Ag<sup>+</sup>) by rotation of the ring about the H axle.<sup>140, 141</sup> Changing the terminal functional groups by carboxylic acids in the H shape linkers Gholami et al. prepared another type of MORF by reaction of the linker with zinc nitrate and copper nitrate.<sup>142, 143</sup>

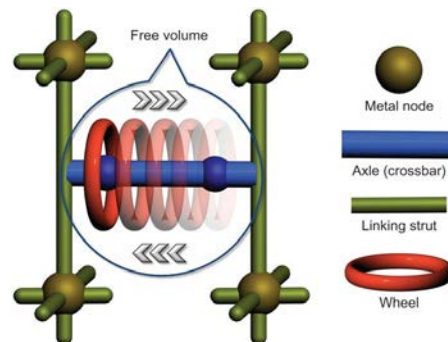


**Fig. 14** MORF materials are commonly constructed from a combination of rigid linking struts (green) and metal nodes (brown). In this design, the components of a MIM-the axle (blue) and wheel (red) of a molecular shuttle-are inserted as a crossbar between the struts. This provides the single wheel component of the MIM with the free volume necessary to undergo unencumbered translational motion between two recognition sites while inside the pores of the MOF. Adapted from K. Zhu, C. A. O'Keefe, V. N. Vukotic, R. W. Schurko and S. J. Loeb, *Nature Chemistry*, 2015, **7**, 514-519. Reprinted by permission from Springer Nature, copyright 2015.

Based on the studies realized with H shape rigid axles, Loeb and co-workers prepared UWDM-4 (Fig. 15), a MOF structure with a molecular shuttle as part of its internal structure. This dynamic material incorporates two benzimidazole recognition sites and a single [24] crown-8 ether. VT <sup>13</sup>C SSNMR experiments demonstrated that the macrocycle of the rotaxane can undergo large-amplitude translational motion along the rigid backbone of the MOF to which it is interlocked.<sup>144, 145</sup>

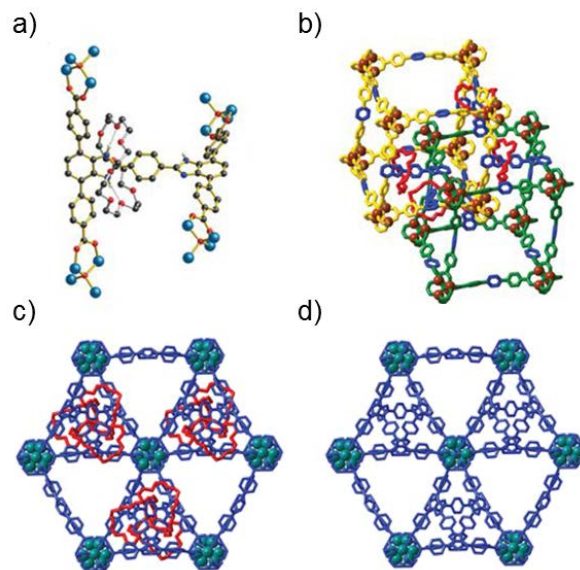


**Fig. 15** Structure of UWDM-4-HBF<sub>4</sub> determined by single-crystal X-ray diffraction. a) Ball-and-stick representation of a single unit of the MIM linker 5 coordinated to four Zn<sub>4</sub>O clusters (only the NH hydrogen atoms are shown for clarity). b) Two

cubes of the lattice formed by the triphenyl struts (green and yellow) with connecting crossbar MIMs (axle in blue and wheel in red); only crossbars actually connecting these two cubes are shown. c) View of the open channels in the lattice down the c axis with macrocycles. d) Same view as in c, with macrocycles omitted. Adapted from K. Zhu, C. A. O'Keefe, V. N. Vukotic, R. W. Schurko and S. J. Loebl, *Nature Chemistry*, 2015, **7**, 514-519. Reprinted by permission from Springer Nature, copyright 2015.

Although the MOFs themselves are porous, the cavity created by the macrocycle ring can be used to form host-guest interactions and capture cationic species within the MOF network. Yaghi, Stoddart and co-workers published in 2012 a modification of a MOF structure with a paraquat dication ( $\text{PQT}^{2+}$ ). In this study was observed how MOF-1001 is able to capture paraquat dication ( $\text{PQT}^{2+}$ ) guests within the macrocycles in a stereoelectronically controlled fashion. This host-guest interaction indicates a charge-transfer between  $\text{PQT}^{2+}$  and crown ether rings without altering its crystallinity (Fig. 16).<sup>116</sup> In the same year, Stoddart et al. designed a MORF (P5A-MOF-1) based on difunctionalized pillar[5]arene ring. This material presented an active domain which is able to uptake neutral and positively charged electron poor aromatic species, leading a colour changes of the crystals (from yellow to deep orange) as consequence of a charge transfer between guest and active domain.<sup>146</sup>

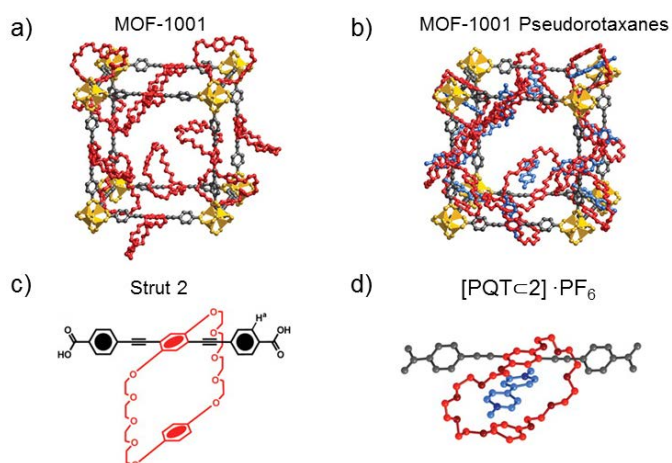


**Fig. 16** a) MOF-1001, b) MOF-1001 pseudorotaxanes, and their molecular analogs c and d). MOF-1001 maintained its crystallinity after docking of  $\text{PQT}^{2+}$ . Adapted from Q. Li, W. Zhang, O. Š. Miljanić, C.-H. Sue, Y.-L. Zhao, L. Liu, C. B. Knobler, J. F. Stoddart and O. M. Yaghi, *Science*, 2009, **325**, 855-859. Reprinted with permission from AAAS, copyright 2009.

Likewise, Coskun et al. reported a coordinated copper [2]pseudorotaxane that reacts with zinc nitrate to form MOF network which is able to undergo electronic switching of some of the copper(I) ions under redox control.<sup>147</sup>

In addition to rotaxanes or pseudorotaxanes, there are MOFs modified with catenanes.<sup>148, 149</sup> For example, reversible redox-switching of bistable [2]catenanes has been retained inside the MOF (Fig. 17), showing that the dynamics of the catenane does not affect the robustness of the MOF. Moreover, this study demonstrates that a catenane can exhibit robust dynamics inside of MOF in the same way as it was mentioned for the rotaxanes.<sup>150</sup>

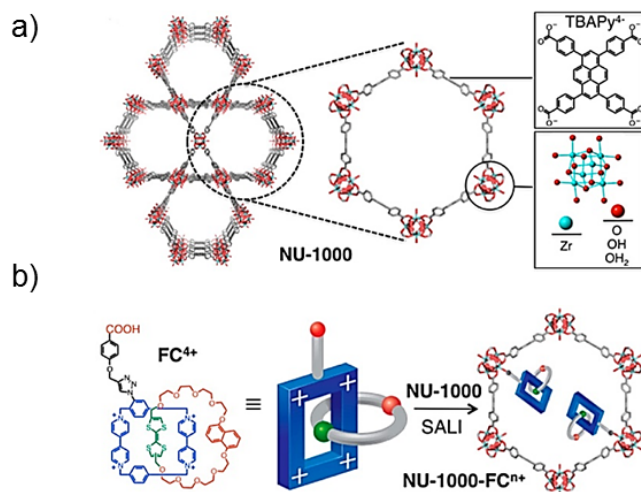


**Fig. 17** a) Structure of NU-1000 (red, oxygen; blue, zirconium; grey, carbon). b) Schematic of the functionalized bistable [2] catenane  $\text{FC}^{4+}$  organized into NU-1000 by the SALI approach. Adapted from Q. Chen, J. Sun, P. Li, I. Hod, P. Z. Moghadam, Z. S. Kean, R. Q. Snurr, J. T. Hupp, O. K. Farha and J. F. Stoddart, *J. Am. Chem. Soc.*, 2016, **138**, 14242-14245 with permission from the American Chemical Society, copyright 2016.

## Mechanically Interlocked Derivatives of Carbon Nanotubes

Single-walled carbon nanotubes (SWNTs) are endowed with one of the most attractive collection of physical properties among nanomaterials:<sup>151</sup> they show extremely high mass-normalised strength<sup>152</sup> and thermal conductivity,<sup>153</sup> metallic carbon nanotubes transport electric current ballistically, while semiconducting nanotubes feature a well-defined bandgap which depends on their chirality.<sup>154</sup> All these properties have made SWNTs the nanomaterial of choice for a variety of applications, from stronger materials to advanced electronic devices.<sup>155</sup> It is however also true that, for most targeted uses, SWNTs have performed disappointingly bad with respect to the initial expectations, often orders of magnitude behind theoretical predictions.<sup>156</sup> A good share of the disenchantment with SWNTs is directly attributable to the problems of hype that all new materials go through, but there are also two main good scientific reasons behind it. First, the challenge of synthesizing monodisperse SWNTs samples with chiral selectivity<sup>157-160</sup> or isolating them from mixtures,<sup>161-164</sup> which has stood in the way of most applications in (opto)electronics –except the few exceptions in which inhomogeneity is actually an advantage, like physically unclonable functions.<sup>165, 166</sup> Second, the tendency of SWNTs to aggregate, that is, to interact strongly with themselves, which in turn means they interact poorly with solvents, hampering processability. This same problem has also frustrated the best use of the mechanical properties of SWNTs in SWNT-polymer composites.<sup>167</sup> Chemical modification of SWNTs has often been proposed as the solution to those problems. To name just a couple of selected examples, the first reports on the covalent functionalization of SWNTs<sup>168</sup> attempted to improve SWNT solubility in common organic sol-

vents.<sup>169</sup> As for the electronic properties, Blanchet and co-workers described a method for the selective addition of fluorinated olefins to metallic nanotubes, suppressing their conductivity and allowing for a mixture of SWNTs to be used as semiconductor material in thin film transition applications.<sup>170</sup> In perfect parallelism, the first studies on the supramolecular chemistry of SWNTs<sup>171</sup> were also directed at improving their solubility, in this case in water.<sup>172-174</sup> Later, noncovalent chemistry has proven as one of the most powerful tools to purify SWNTs to obtain single-chirality,<sup>162,175</sup> and even single handedness,<sup>176-178</sup> samples. With these precedents, interfacing SWNTs and molecules through mechanical links seems particularly attractive.

The first examples of mechanically interlocked molecules featuring nanocarbon molecules were focused on the soluble molecular fullerenes, mainly using them as stoppers,<sup>179-183</sup> and more recently as templates in the thread.<sup>184, 185</sup> As for SWNTs, the first combinations of MIMs and nanotubes were described by the groups of Stoddart and Heath, based on the noncovalent sidewall modification with catenane<sup>186</sup> or pseudorotaxane<sup>187</sup> architectures (Fig. 18).<sup>171</sup>

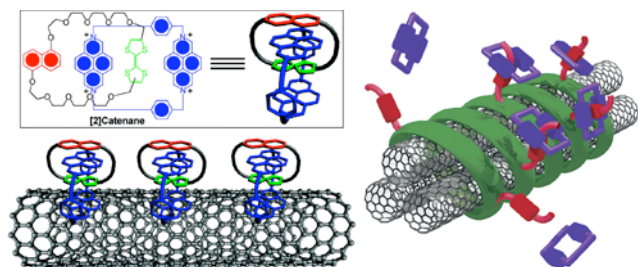


**Fig. 18.** Noncovalent sidewall functionalisation of SWNTs with catenanes (left) and pseudorotaxanes (right) described by the groups of Stoddart and Heath.<sup>186, 187</sup> Adapted from: M. R. Diehl, D. W. Steuerman, H.-R. Tseng, S. A. Vignon, A. Star, P. C. Celestre, J. F. Stoddart and J. R. Heath, *ChemPhysChem*, 2003, **4**, 1335-1339 and A. Star, Y. Liu, K. Grant, L. Ridvan, J. F. Stoddart, D. W. Steuerman, M. R. Diehl, A. Boukai and J. R. Heath, *Macromolecules*, 2003, **36**, 553-560 with permission from Wiley-VCH, copyright 2003, and the American Chemical Society, copyright 2003, respectively.

The extreme aspect ratio of SWNTs makes them suitable for their threading through organic macrocycles to form [n]rotaxane-type<sup>188</sup> mechanically interlocked derivatives of SWNTs (MINTs, Fig. 19). Initially, one can expect to get to a best-of-both-worlds situation, conserving a degree of stability comparable to covalent modifications, but without saturation of any  $sp^2$  Cs, and therefore preserving (or hopefully improving!) the outstanding physical properties of SWNTs. The idea was based on a “clipping” strategy, where we would use U-shaped molecules featuring two units of a recognition fragment for SWNTs (for example, pyrene in Fig. 19a), connected through an aromatic spacer and finally decorated with alkene-terminated alkyl chains. With this molecular design, our strategy is based on two sequential steps, first a supramolecular event: we expect the U-shapes to be able to associate individualised segments of SWNTs. Secondly, once the U-shapes are associated, we can close them around the SWNTs to form the rotaxane-type MINTs using ring-closing metathesis (RCM). Finally, we rely in extensive washings with solvents in which catalyst, U-shapes, non-interlocked

macrocycles, etc. are very soluble, to remove any material that is not very tightly bound to the SWNTs.<sup>189</sup>

The supramolecular equilibrium is governed by an association constant ( $K_a$ ) that can be measured using a relatively simple titration method, and is the solvents that we use to form MINTs (typically tetrachlorethane, TCE) and at room temperature is a respectable  $K_a = 10^3-10^4 \text{ M}^{-1}$ .<sup>190, 191</sup> This implies that at the concentrations we typically run the MINT-forming reaction (ca. 0.5 mM), more than 50% of our U-shapes are associated to the SWNTs at the beginning of the reaction. A major concern when using Grubb’s catalysts with bisalkene molecules is the competitive oligomerization reaction, which can take place by reaction between two U-shapes instead of RCM. Oligomers formed this way would associate very strongly to SWNTs, and are potential impurities in the final product. To analyse the role of oligomerisation, we investigated the kinetics of the MINT forming reaction, and found that could be well fitted to pseudo first order kinetics to afford  $k_{RCM} = 7.4 \times 10^{-5} \text{ s}^{-1}$ , in line with RCM (and not oligomerisation, which would be second order) being the major mechanism. Moreover, by increasing the amount of Grubb’s catalyst,<sup>192</sup> or using specific SWNT recognition motifs under certain conditions,<sup>193</sup> we can force the formation of significant amounts of oligomers, which are perfectly distinguishable from MINTs through simple thermogravimetric analysis. With these simple analyses we can ascertain that the majority of the functionalisation in our samples must correspond to rotaxane-type MINTs. Thanks to the tremendous advances in aberration-corrected high-resolution electron microscopy at sufficiently low-voltage to prevent immediate damage to the organic macrocycles, we were also able to image MINTs with close to atomic resolution Fig. 19c.

An alternative synthetic pathway, based on direct threading of SWNTs through rigid cycloparaphenyleneacetylene (CPPA) macrocycles was recently reported by Miki, Ohe, and co-workers.<sup>194</sup> In this “ring-tossing” strategy, the authors directly mixed CPPAs and SWNTs in *o*-dichlorobenzene, to obtain the complexes. Through comparison between the fit of the CPPA cavity and the SWNT diameter and the amount of complex obtained, and careful analysis of the TGA data, the authors conclude that both tube-in-ring and tube-on-ring complexes are present in most cases in the final product, except in cases where the fit is particularly tight, like that between the [9] CPPA shown in Fig. 16b (1.89 nm cavity) and SWNTs of 1.1-1.4 nm diameter, where the tube-in-ring binding mode predominates.

Finally, the templated formation of self-assembled hydrogen bonded macrocycles around SWNTs has also been described by González-Rodríguez and co-workers.<sup>195</sup>

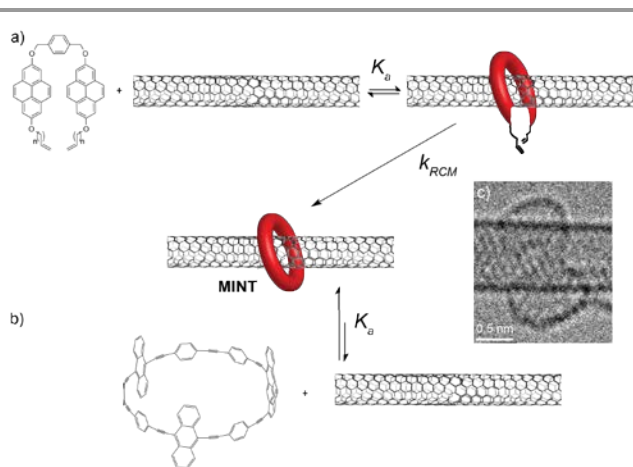


**Fig. 19** Synthetic pathways towards MINTs. a) Clipping strategy, based on association of SWNTs by alkene-terminated U-shapes featuring recognition units for SWNTs (in this case illustrated with pyrene) followed by RCM.<sup>189</sup> b) A pre-formed rigid CPPA macrocycle is directly threaded by the SWNTs under specific conditions, as described by Miki, Ohe and co-workers.<sup>194</sup> c) HRTEM of a MINT synthesised by Pérez and co-workers.<sup>196</sup>

Although these are, to the best of our knowledge, “the first” examples where rotaxane-type derivatives of SWNTs have been targeted and unambiguously characterised, as usual, there are no firsts in science. Before we set sail to navigate these seas, others had probably touched land already. For example, in 2005, Dieckmann and co-workers had reported the diameter-selective solubilisation of SWNTs using peptide macrocycles reversibly formed using disulfide chemistry, in which their proposed main mode of action was encapsulation of the SWNTs within the macrocycles.<sup>197</sup> That same year, Stoddart and co-workers described the formation of “acyclic and/or cyclic adducts *on or around* the side walls of SWNTs” using Pd coordination of porphyrin fragments.<sup>198</sup> The formation of covalent porphyrinic networks around MWNTs described by Campidelli and co-workers,<sup>199</sup> and, more recently, the encapsulation of SWNTs within peptide  $\beta$ -barrels by Kruss and co-workers,<sup>200</sup> can also be considered close relatives of MINTs.

With the synthetic tools towards MINTs already in place, we are now exploring if the mechanical bond is indeed a useful addition to the chemistry toolkit for modification of SWNTs. To this end, the structural flexibility provided by our clipping approach is crucial. In our hands, this simple design strategy has so far worked for any molecular fragment known to associate SWNTs efficiently, including,  $\pi$ -extended derivatives of tetrathiafulvalene (exTTF),<sup>201</sup> pyrene,<sup>202</sup> naphthalene diimides,<sup>193</sup> porphyrins,<sup>203</sup> and anthraquinone.<sup>200</sup> Moreover, substituents on the aromatic spacer,<sup>193</sup> and oligo ethyleneglycol alkene terminated spacers<sup>204</sup> are also tolerated.

An ideal tool for the chemical modification of SWNTs should allow the tuning of surface and electronic properties. In collaboration with the groups led by Rubio, Guldi and Lorenzo, we carried out an extensive experimental and theoretical investigation of the influence of linking exTTF electron donors to SWNTs through mechanical links, in comparison with non-interlocked supramolecular model systems.<sup>205</sup> Our results showed that, in the

ground-state, the degree of charge-transfer between exTTF and SWNTs is negligible, whereas upon photoexcitation, rapid electron transfer from exTTF to the SWNTs takes place. The rates of transfer and recombination are significantly different in the interlocked and non-interlocked compounds, showing the unique effect of the MINT-type modification. Later, we have found similar conclusions for porphyrin-based MINTs.<sup>203</sup>

From a more practical point of view, we exploited the tuning of the electronic properties of SWNTs to modify their catalytic properties. In particular, we investigated the catalytic role of MINTs in the reduction of nitroarenes with hydrazine, a reaction in which SWNTs are known to act both as an adsorbent and as an electron reservoir. Comparing the catalytic activity of pristine SWNTs, and MINTs with electron donor (MINT-exTTF), acceptor (MINT-AQ), or electronically neutral (MINT-pyr) macrocycles, we established a clear relationship between the expected electronic density at the SWNT surface and the catalytic activity.<sup>196</sup> In particular, the catalytic activity increases with electron density on the SWNT. That is, the electron rich(er) MINT-exTTF performs significantly better as catalyst than the pristine SWNTs (black in Fig. 20), which in turn show similar activity as MINT-pyr, and much better than the electron poor(er) MINT-AQ (green in Fig. 20). This catalyst regulation strategy presents a unique combination of the properties observed in the natural up/down regulation of enzymes: the link between the effectors (the macrocycles) and the catalyst (the nanotubes) is noncovalent, yet stable thanks to the mechanical link, and its effect is remote but not allosteric, since it does not change the structure of the active site (the surface of the nanotube).

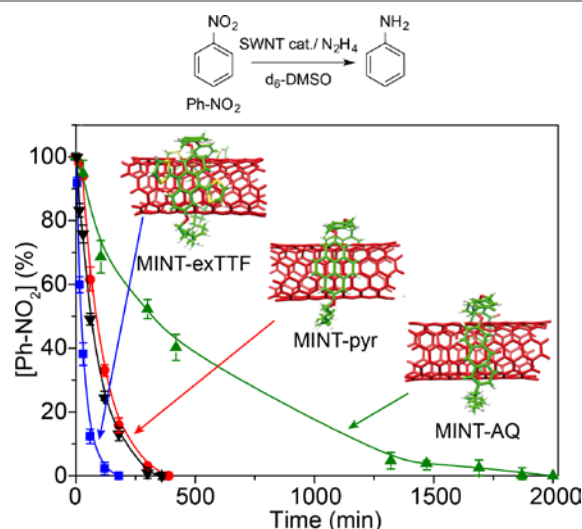


**Fig. 20** Regulation of SWNT catalyst activity towards the reduction of nitroarenes, using macrocycles of different electronic character. The electron-rich MINT-exTTF (blue) is a better catalyst than pristine SWNTs (black) or electronically neutral MINT-pyr (red), while the electron-poor MINT-AQ (green) shows considerably decreased activity.<sup>196</sup>

With regards to the surface properties, the tendency of SWNTs to aggregate is a problem in many areas, but perhaps particularly so in their use as polymers fillers. The extraordinary mechanical properties of SWNT immediately attracted the attention of the

material chemist for their potential use for the reinforcement of polymers.<sup>167</sup> However, the results in this area have been particularly disappointing due to the tendency of SWNTs to interact with themselves and self-aggregate, which results in a poor interaction with the polymer and therefore suboptimal load-transfer.<sup>206</sup> Encapsulating the SWNTs within organic macrocycles, to form MINTs, seems a plausible strategy to aid in individualisation and an enhanced polymer SWNT interaction. With this hypothesis in mind, we tested the mechanical properties of electrospun polystyrene fibers doped with 0.01 wt % MINTs prepared from three different types of SWNTs and two different macrocycles, and compared the mechanical properties of the nanocomposites with pristine SWNTs and supramolecular complexes of identical chemical composition as the MINTs (Fig. 21).<sup>207</sup>

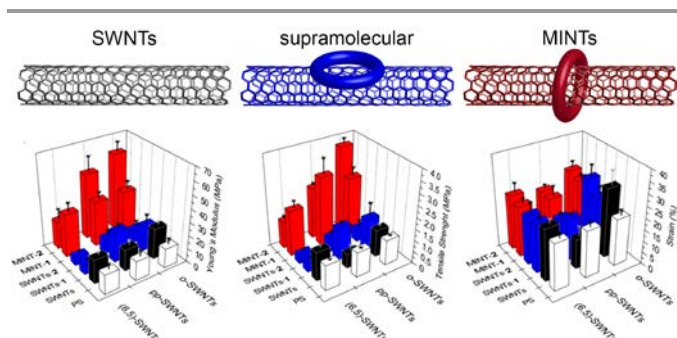


**Fig. 21** MINTs (red) behave as superior fillers when combined with pristine SWNTs (grey/black) or adequate supramolecular controls (blue). Significant improvements in Young's modulus (left) and tensile strength (middle) were observed systematically for MINT-reinforced polystyrene fibers.<sup>208</sup>

## Conclusions

The birth of a new type of bond brings the biggest possible window of opportunity for the chemical sciences. This is the case for the mechanical link, too. The chemistry of “small” mechanically-interlocked molecules has allowed to produce some of the most intricate structures<sup>208, 209</sup> and fascinating synthetic molecular devices.<sup>210-212</sup> Meanwhile, the application of the mechanical bond to materials science has just started to bloom.<sup>213</sup> In this review, we have overviewed the synthetic pathways to polycatenanes, polyrotaxanes, MORFs and MINTs, which are already in place. Other mechanised structures in the frontier of materials science, like mesostructured silica particles<sup>214, 215</sup> and metallic nanoparticles<sup>216, 217</sup> have also been studied, but are not covered here. In some fields, proof-of-concept of the first practical applications of mechanically interlocked materials have already been produced, influencing key fields like energy storage,<sup>106</sup> stronger plastics,<sup>207</sup> or nanomedicine.<sup>65</sup> Most of these already benefit from the inherent dynamic properties of the mechanical bond, but the exquisite control over submolecular motion that is now commonplace in small-molecule MIMs remains perhaps the grandest challenge for this area of research. When our synthetic mastery allows us to access complete control over stimuli-controlled submolecular motion in mechanically interlocked materials we should have access to smart-materials with the potential to revolutionise materials science.

## Acknowledgements

We acknowledge funding for the European Union (ERC-StG-MINT 307609), the Ministerio de Economía y Competitividad (CTQ2014-60541-P and CTQ2017-86060-P), and the Comunidad de Madrid (MAD2D-CM program S2013/MIT-3007). IMDEA Nanociencia acknowledges support from the “Severo Ochoa” Programme for Centres of Excellence in R&D (MINECO, Grant SEV-2016-0686)

## Notes and references

<sup>a</sup> IMDEA Nanociencia, Faraday 9, Campus UAM, 28049 Madrid, Spain; E-mail: emilio.perez@imdea.org

- H. L. Frisch and E. Wasserman, *J. Am. Chem. Soc.*, 1961, **83**, 3789-3795.
- G. Schill, *Catenanes, Rotaxanes and Knots*, Academic Press, New York, 1971.
- R. Brückner, *Eur. J. Org. Chem.*, 2019, 3289-3319.
- E. Wasserman, *J. Am. Chem. Soc.*, 1960, **82**, 4433-4434.
- G. Schill and A. Lüttringhaus, *Angew. Chem. Int. Ed.*, 1964, **3**, 546-547.
- I. T. Harrison and S. Harrison, *J. Am. Chem. Soc.*, 1967, **89**, 5723-5724.
- C. O. Dietrich-Buchecker, J. P. Sauvage and J. M. Kern, *J. Am. Chem. Soc.*, 1984, **106**, 3043-3045.
- C. O. Dietrich-Buchecker, J. P. Sauvage and J. P. Kintzinger, *Tetrahedron Lett.*, 1983, **24**, 5095-5098.
- P. R. Ashton, I. Baxter, M. C. T. Fyfe, F. M. Raymo, N. Spencer, J. F. Stoddart, A. J. P. White and D. J. Williams, *J. Am. Chem. Soc.*, 1998, **120**, 2297-2307.
- A. Affeld, G. M. Hubner, C. Seel and C. A. Schalley, *Eur. J. Org. Chem.*, 2001, 2877-2890.
- D. M. Walba, *Tetrahedron*, 1985, **41**, 3161-3212.
- G. A. Breault, C. A. Hunter and P. C. Mayers, *Tetrahedron*, 1999, **55**, 5265-5293.
- L. D. Movsisyan, M. Franz, F. Hampel, A. L. Thompson, R. R. Tykwinski and H. L. Anderson, *J. Am. Chem. Soc.*, 2016, **138**, 1366-1376.
- M. Franz, J. A. Januszewski, D. Wendinger, C. Neiss, L. D. Movsisyan, F. Hampel, H. L. Anderson, A. Goerling and R. R. Tykwinski, *Angew. Chem., Int. Ed.*, 2015, **54**, 6645-6649.
- L. D. Movsisyan, D. V. Kondratuk, M. Franz, A. L. Thompson, R. R. Tykwinski and H. L. Anderson, *Org. Lett.*, 2012, **14**, 3424-3426.
- J. M. Baumes, J. J. Gassensmith, J. Giblin, J.-J. Lee, A. G. White, W. J. Culligan, W. M. Leevy, M. Kuno and B. D. Smith, *Nat. Chem.*, 2010, **2**, 1025-1030.
- J. R. Johnson, N. Fu, E. Arunkumar, W. M. Leevy, S. T. Gammon, D. Piwnica-Worms and B. D. Smith, *Angew. Chem., Int. Ed.*, 2007, **46**, 5528-5531, S5528/S521-S5528/S515.
- E. Arunkumar, C. C. Forbes, B. C. Noll and B. D. Smith, *J. Am. Chem. Soc.*, 2005, **127**, 3288-3289.
- J.-P. Sauvage, *Angew. Chem., Int. Ed.*, 2017, **56**, 11080-11093.
- J. F. Stoddart, *Angew. Chem., Int. Ed.*, 2017, **56**, 11094-11125.
- B. L. Feringa, *Angew. Chem., Int. Ed.*, 2017, **56**, 11060-11078.
- E. A. Neal and S. M. Goldup, *Chem. Commun.*, 2014, **50**, 5128-5142.
- E. M. G. Jamieson, F. Modicom and S. M. Goldup, *Chem. Soc. Rev.*, 2018, **47**, 5266-5311.
- J. M. Abendroth, P. S. Weiss, C. J. Barrett, O. S. Bushuyev, C. J. Barrett and P. S. Weiss, *ACS Nano*, 2015, **9**, 7746-7768.
- J. Rotzler and M. Mayor, *Chem. Soc. Rev.*, 2013, **42**, 44-62.
- C. J. Bruns and J. F. Stoddart, *Top. Curr. Chem.*, 2012, **323**, 19-27.
- G. Barin, A. Coskun, M. M. G. Fouda and J. F. Stoddart, *ChemPlusChem*, 2012, **77**, 159-185.
- S. Kassem, T. van Leeuwen, A. S. Lubbe, M. R. Wilson, B. L. Feringa and D. A. Leigh, *Chem. Soc. Rev.*, 2017, **46**, 2592-2621.
- D. A. Leigh, *Angew. Chem., Int. Ed.*, 2016, **55**, 14506-14508.
- G. Gil-Ramirez, D. A. Leigh and A. J. Stephens, *Angew. Chem., Int. Ed.*, 2015, **54**, 6110-6150.

31. S. Erbas-Cakmak, D. A. Leigh, C. T. McTernan and A. L. Nussbaumer, *Chem. Rev.*, 2015, **115**, 10081-10206.
32. V. Blanco, D. A. Leigh and V. Marcos, *Chem. Soc. Rev.*, 2015, **44**, 5341-5370.
33. K. D. Haenni and D. A. Leigh, *Chem. Soc. Rev.*, 2010, **39**, 1240-1251.
34. J. E. Beves and D. A. Leigh, *Nat. Chem.*, 2010, **2**, 708-710.
35. J. D. Crowley, S. M. Goldup, A.-L. Lee, D. A. Leigh and R. T. McBurney, *Chem. Soc. Rev.*, 2009, **38**, 1530-1541.
36. E. R. Kay, D. A. Leigh and F. Zerbetto, *Angew. Chem., Int. Ed.*, 2007, **46**, 72-191.
37. F. Huang and E. V. Anslyn, *Chem. Rev.*, 2015, **115**, 6999-7000.
38. J. E. M. Lewis, P. D. Beer, S. J. Loeb and S. M. Goldup, *Chem. Soc. Rev.*, 2017, **46**, 2577-2591.
39. H. W. Gibson, M. C. Bheda and P. T. Engen, *Prog. Polym. Sci.*, 1994, **19**, 843-945.
40. Z. Niu and H. W. Gibson, *Chem. Rev.*, 2009, **109**, 6024-6046.
41. C. Gong and H. W. Gibson, *Curr. Opin. Solid St. M.*, 1997, **2**, 647-652.
42. F. M. Raymo and J. F. Stoddart, *Chem. Rev.*, 1999, **99**, 1643-1664.
43. A. Harada, *Acta Polym.*, 1998, **49**, 3-17.
44. A. Harada, A. Hashidzume, H. Yamaguchi and Y. Takashima, *Chem. Rev.*, 2009, **109**, 5974-6023.
45. T. Takata, N. Kihara and Y. Furusho, in *Polymer Synthesis*, Springer Berlin Heidelberg, Berlin, Heidelberg, 2004, pp. 1-75.
46. J.-L. Weidmann, J.-M. Kern, J.-P. Sauvage, D. Muscat, S. Mullins, W. Köhler, C. Rosenauer, H. J. Räder, K. Martin and Y. Geerts, *Chem. Eur. J.*, 1999, **5**, 1841-1851.
47. T. Pakula and K. Jeszka, *Macromolecules*, 1999, **32**, 6821-6830.
48. P. M. Rauscher, S. J. Rowan and J. J. de Pablo, *ACS Macro Lett.*, 2018, **7**, 938-943.
49. J.-L. Weidmann, J.-M. Kern, J.-P. Sauvage, Y. Geerts, D. Muscat and K. Müllen, *Chem. Commun.*, 1996, 1243-1244.
50. C. Hamers, F. M. Raymo and J. F. Stoddart, *Eur. J. Org. Chem.*, 1998, 2109-2117.
51. D. Muscat, W. Köhler, H. J. Räder, K. Martin, S. Mullins, B. Müller, K. Müllen and Y. Geerts, *Macromolecules*, 1999, **32**, 1737-1745.
52. N. Watanabe, Y. Ikari, N. Kihara and T. Takata, *Macromolecules*, 2004, **37**, 6663-6666.
53. C. Hamers, O. Kocian, F. M. Raymo and J. F. Stoddart, *Adv. Mater.*, 1998, **10**, 1366-1369.
54. C.-A. Fustin, C. Bailly, G. J. Clarkson, P. De Groot, T. H. Galow, D. A. Leigh, D. Robertson, A. M. Z. Slawin and J. K. Y. Wong, *J. Am. Chem. Soc.*, 2003, **125**, 2200-2207.
55. B. N. Ahamed, P. Van Velthem, K. Robeyns and C.-A. Fustin, *ACS Macro Lett.*, 2017, **6**, 468-472.
56. M. A. Olson, A. B. Braunschweig, L. Fang, T. Ikeda, R. Klajn, A. Trabolsi, P. J. Wesson, D. Benítez, C. A. Mirkin, B. A. Grzybowski and J. F. Stoddart, *Angew. Chem. Int. Ed.*, 2009, **48**, 1792-1797.
57. P.-F. Cao, J. D. Mangadlao, A. de Leon, Z. Su and R. C. Advincula, *Macromolecules*, 2015, **48**, 3825-3833.
58. J. A. Berrocal, L. M. Pitet, M. M. L. Nieuwenhuizen, L. Mandolini, E. W. Meijer and S. Di Stefano, *Macromolecules*, 2015, **48**, 1358-1363.
59. D. B. Amabilino, P. R. Ashton, A. S. Reder, N. Spencer and J. F. Stoddart, *Angew. Chem. Int. Ed.*, 1994, **33**, 1286-1290.
60. H. Iwamoto, S. Tafuku, Y. Sato, W. Takizawa, W. Katagiri, E. Tayama, E. Hasegawa, Y. Fukazawa and T. Haino, *Chem. Commun.*, 2016, **52**, 319-322.
61. D. B. Amabilino, P. R. Ashton, S. E. Boyd, J. Y. Lee, S. Menzer, J. F. Stoddart and D. J. Williams, *Angew. Chem., Int. Ed. Engl.*, 1997, **36**, 2070-2072.
62. Q. Wu, P. M. Rauscher, G. Lang, R. J. Wojtecki, J. J. de Pablo, M. J. A. Hore and S. J. Rowan, *Science*, 2017, **358**, 1434-1439.
63. T. J. Kidd, T. J. A. Loontjens, D. A. Leigh and J. K. Y. Wong, *Angew. Chem., Int. Ed.*, 2003, **42**, 3379-3383.
64. K. Kim, *Chem. Soc. Rev.*, 2002, **31**, 96-107.
65. L. Fang, M. A. Olson, D. Benítez, E. Tkatchouk, W. A. Goddard III and J. F. Stoddart, *Chem. Soc. Rev.*, 2010, **39**, 17-29.
66. Y. Suzaki, T. Taira and K. Osakada, *J. Mater. Chem.*, 2011, **21**, 930-938.
67. B.-H. H. a. A. M. G. Wenz, *Chem. Rev.*, 2006, **106**, 782-817.
68. P.-G. de Gennes, *Physica A*, 1999, **271**, 231-237.
69. Y. Okumura and K. Ito, *Adv. Mater.*, 2001, **13**, 485-487.
70. T. Karino, Y. Okumura, K. Ito and M. Shibayama, *Macromolecules*, 2004, **37**, 6177-6182.
71. G. Fleury, G. Schlatter, C. Brochon and G. Hadziioannou, *Polymer*, 2005, **46**, 8494-8501.
72. G. Fleury, G. Schlatter, C. Brochon, C. Travelet, A. Lapp, P. Lindner and G. Hadziioannou, *Macromolecules*, 2007, **40**, 535-543.
73. A. B. Imran, T. Seki, K. Ito and Y. Takeoka, *Macromolecules*, 2010, **43**, 1975-1980.
74. K. Kato, K. Inoue, M. Kidowaki and K. Ito, *Macromolecules*, 2009, **42**, 7129-7136.
75. T. Sakai, H. Murayama, S. Nagano, Y. Takeoka, M. Kidowaki, K. Ito and T. Seki, *Adv. Mater.*, 2007, **19**, 2023-2025.
76. H. Murayama, A. B. Imran, S. Nagano, T. Seki, M. Kidowaki, K. Ito and Y. Takeoka, *Macromolecules*, 2008, **41**, 1808-1814.
77. K. Ito, *Polym. J.*, 2011, **44**, 38.
78. J. Araki and K. Ito, *Polymer*, 2007, **48**, 7139-7144.
79. Y. Bitoh, N. Akuzawa, K. Urayama, T. Takigawa, M. Kidowaki and K. Ito, *Macromolecules*, 2011, **44**, 8661-8667.
80. J. Sawada, D. Aoki, S. Uchida, H. Otsuka and T. Takata, *ACS Macro Lett.*, 2015, **4**, 598-601.
81. A. Bin Imran, K. Esaki, H. Gotoh, T. Seki, K. Ito, Y. Sakai and Y. Takeoka, in *Nat. Commun.*, 2014, vol. 5, p. 5124.
82. K. Kato, K. Karube, N. Nakamura and K. Ito, *Polym. Chem.*, 2015, **6**, 2241-2248.
83. K. Kato, T. Mizusawa, H. Yokoyama and K. Ito, *J. Phys. Chem. Lett.*, 2015, **6**, 4043-4048.
84. K. Kato, T. Mizusawa, H. Yokoyama and K. Ito, *J. Phys. Chem. C*, 2017, **121**, 1861-1869.
85. K. Kato, K. Nemoto, K. Mayumi, H. Yokoyama and K. Ito, *ACS Appl. Mater. Inter.*, 2017, **9**, 32436-32440.
86. S. Uenuma, R. Maeda, K. Kato, K. Mayumi, H. Yokoyama and K. Ito, *ACS Macro Lett.*, 2019, **8**, 140-144.
87. H. Taneda, A. Shundo, H. Matsuno and K. Tanaka, *Langmuir*, 2018, **34**, 709-714.
88. T. Arai, K. Jang, Y. Koyama, S. Asai and T. Takata, *Chem. Eur. J.*, 2013, **19**, 5917-5923.
89. M. Ogawa, H. Sogawa, Y. Koyama and T. Takata, *Polymer Journal*, 2015, **47**, 580.
90. K. Iijima, D. Aoki, H. Otsuka and T. Takata, *Polymer*, 2017, **128**, 392-396.
91. K. Jang, K. Iijima, Y. Koyama, S. Uchida, S. Asai and T. Takata, *Polymer*, 2017, **128**, 379-385.
92. M. D. Hager, P. Greil, C. Leyens, S. van der Zwaag and U. S. Schubert, *Adv. Mater.*, 2010, **22**, 5424-5430.
93. D. Habault, H. Zhang and Y. Zhao, *Chem. Soc. Rev.*, 2013, **42**, 7244-7256.
94. Y. Yang and M. W. Urban, *Chem. Soc. Rev.*, 2013, **42**, 7446-7467.
95. C. Wang, N. Liu, R. Allen, J. B. H. Tok, Y. Wu, F. Zhang, Y. Chen and Z. Bao, *Adv. Mater.*, 2013, **25**, 5785-5790.
96. W. Xu, L.-B. Huang and J. Hao, *Nano Energy*, 2017, **40**, 399-407.
97. F. Herbst, D. Döhler, P. Michael and W. H. Binder, *Macromol. Rapid. Commun.*, 2013, **34**, 203-220.
98. G. M. L. van Gemert, J. W. Peeters, S. H. M. Soentjens, H. M. Janssen and A. W. Bosman, *Macromol. Chem. Phys.*, 2012, **213**, 234-242.
99. T. Aida, E. W. Meijer and S. I. Stupp, *Science*, 2012, **335**, 813-817.
100. M. Nakahata, Y. Takashima, H. Yamaguchi and A. Harada, *Nat. Commun.*, 2011, **2**, 511.
101. M. Nakahata, S. Mori, Y. Takashima, H. Yamaguchi and A. Harada, *Chem*, 2016, **1**, 766-775.
102. Y. Takashima, S. Hatanaka, M. Otsubo, M. Nakahata, T. Kakuta, A. Hashidzume, H. Yamaguchi and A. Harada, *Nat. Commun.*, 2012, **3**, 1270.
103. Y.-L. Zhao and J. F. Stoddart, *Langmuir*, 2009, **25**, 8442-8446.
104. I. Tomatsu, A. Hashidzume and A. Harada, *J. Am. Chem. Soc.*, 2006, **128**, 2226-2227.
105. S. Tamesue, Y. Takashima, H. Yamaguchi, S. Shinkai and A. Harada, *Angew. Chem. Int. Ed.*, 2010, **49**, 7461-7464.
106. T.-W. Kwon, J. W. Choi and A. Coskun, *Chem. Soc. Rev.*, 2018, **47**, 2145-2164.

107. J. Li, R. B. Lewis and J. R. Dahn, *Electrochem. Solid St. Lett.*, 2007, **10**, 17-20
108. I. Kovalenko, B. Zdyrko, A. Magasinski, B. Hertzberg, Z. Milicev, R. Burtovyy, I. Luzinov and G. Yushin, *Science*, 2011, **334**, 75-79.
109. S. Choi, T.-w. Kwon, A. Coskun and J. W. Choi, *Science*, 2017, **357**, 279-283.
110. X. H. Liu, L. Zhong, S. Huang, S. X. Mao, T. Zhu and J. Y. Huang, *ACS Nano.*, 2012, **6**, 1522-1531.
111. U. Kasavajjula, C. Wang and A. J. Appleby, *J. Power Sources*, 2007, **163**, 1003-1039.
112. H. Furukawa, K. E. Cordova, M. O'Keefe and O. M. Yaghi, *Science*, 2013, **341**, 1230444.
113. S. Yuan, L. Feng, K. Wang, J. Pang, M. Bosch, C. Lollar, Y. Sun, J. Qin, X. Yang, P. Zhang, Q. Wang, L. Zou, Y. Zhang, L. Zhang, Y. Fang, J. Li and H.-C. Zhou, *Adv. Mater.*, 2018, **30**, 1704303.
114. S. L. James, *Chem. Soc. Rev.*, 2003, **32**, 276-288.
115. S. Dang, Q.-L. Zhu and Q. xu, *Nat. Rev. Mater.*, 2017, **3**, 1-14
116. Q. Li, W. Zhang, O. Š. Miljanić, C.-H. Sue, Y.-L. Zhao, L. Liu, C. B. Knobler, J. F. Stoddart and O. M. Yaghi, *Science*, 2009, **325**, 855-859.
117. R. A. Smaldone, R. S. Forgan, H. Furukawa, J. J. Gassensmith, A. M. Z. Slawin, O. M. Yaghi and J. F. Stoddart, *Angew. Chem. Int. Ed.*, 2010, **49**, 8630-8634.
118. J. Lee, O. K. Farha, J. Roberts, K. A. Scheidt, S. T. Nguyen and J. T. Hupp, *Chem. Soc. Rev.*, 2009, **38**, 1450-1459.
119. L. Jiao, Y. Wang, H.-L. Jiang and Q. Xu, *Adv. Mater.*, 2018, **30**, 1703663.
120. A. Dhakshinamoorthy, Z. Li and H. Garcia, *Chem. Soc. Rev.*, 2018, **47**, 8134-8172.
121. A. Tomita and M. Sano, *Inorg. Chem.*, 2000, **39**, 200-205.
122. M. P. Suh, H. J. Park, T. K. Prasad and D.-W. Lim, *Chem. Rev.*, 2012, **112**, 782-835.
123. C.-Y. Sun, C. Qin, C.-G. Wang, Z.-M. Su, S. Wang, X.-L. Wang, G.-S. Yang, K.-Z. Shao, Y.-Q. Lan and E.-B. Wang, *Adv. Mater.*, 2011, **23**, 5629-5632.
124. P. Horcajada, C. Serre, G. Maurin, N. A. Ramsahye, F. Balas, M. Vallet-Regí, M. Sebban, F. Taulelle and G. Férey, *J. Am. Chem. Soc.*, 2008, **130**, 6774-6780.
125. W. Cai, J. Wang, C. Chu, W. Chen, C. Wu and G. Liu, *Adv. Sci.*, 2019, **6**, 1801526.
126. T. Simon-Yarza, A. Miellecarek, P. Couvreur and C. Serre, *Adv. Mater.*, 2018, **30**, 1870281.
127. S. Rojas, T. Baati, L. Njim, L. Manchego, F. Neffati, N. Abdeljelil, S. Saguem, C. Serre, M. F. Najjar, A. Zakhama and P. Horcajada, *J. Am. Chem. Soc.*, 2018, **140**, 9581-9586.
128. K. Lu, T. Aung, N. Guo, R. Weichselbaum and W. Lin, *Adv. Mater.*, 2018, **30**, 1707634.
129. Y. Chen, P. Li, J. A. Modica, R. J. Drout and O. K. Farha, *J. Am. Chem. Soc.*, 2018, **140**, 5678-5681.
130. H. Deng, M. A. Olson, J. F. Stoddart and O. M. Yaghi, *Nat. Chem.*, 2010, **2**, 439-443.
131. S. J. Loeb, *Chem. Soc. Rev.*, 2007, **36**, 226-235.
132. S. J. Loeb, *Chem. Commun.*, 2005, 1511-1518.
133. E. Lee, J. Heo and K. Kim, *Angew. Chem. Int. Ed.*, 2000, **39**, 2699-2701.
134. D. J. Hoffart and S. J. Loeb, *Angew. Chem. Int. Ed.*, 2005, **44**, 901-904.
135. R. Krauss, H.-G. Weinig, M. Seydack, J. Bendig and U. Koert, *Angew. Chem., Int. Ed.*, 2000, **39**, 1835-1837.
136. V. N. Vukotic, K. J. Harris, K. Zhu, R. W. Schurko and S. J. Loeb, *Nat. Chem.*, 2012, **4**, 456-460.
137. V. N. Vukotic, C. A. O'Keefe, K. Zhu, K. J. Harris, C. To, R. W. Schurko and S. J. Loeb, *J. Am. Chem. Soc.*, 2015, **137**, 9643-9651.
138. K. Zhu, V. N. Vukotic, C. A. O'Keefe, R. W. Schurko and S. J. Loeb, *J. Am. Chem. Soc.*, 2014, **136**, 7403-7409.
139. K. Zhu, V. N. Vukotic and S. J. Loeb, *Angew. Chem. Int. Ed.*, 2012, **51**, 2168-2172.
140. G. Baggi and S. J. Loeb, *Angew. Chem. Int. Ed.*, 2016, **55**, 12533-12537.
141. G. Baggi and S. J. Loeb, *Chem. Eur. J.*, 2017, **23**, 14163-14166.
142. G. Gholami, K. Zhu, J. S. Ward, P. E. Kruger and S. J. Loeb, *Eur. J. Inorg. Chem.*, 2016, 4524-4529.
143. G. Gholami, G. Baggi, K. Zhu and S. J. Loeb, *Dalton Trans.*, 2017, **46**, 2462-2470.
144. K. Zhu, C. A. O'Keefe, V. N. Vukotic, R. W. Schurko and S. J. Loeb, *Nat. Chem.*, 2015, **7**, 514-519.
145. M. A. Olson, *Nat. Chem.*, 2015, **7**, 470-471.
146. N. L. Strutt, D. Fairen-Jimenez, J. Iehl, M. B. Lalonde, R. Q. Snurr, O. K. Farha, J. T. Hupp and J. F. Stoddart, *J. Am. Chem. Soc.*, 2012, **134**, 17436-17439.
147. A. Coskun, M. Hmadeh, G. Barin, F. Gándara, Q. Li, E. Choi, N. L. Strutt, D. B. Cordes, A. M. Z. Slawin, J. F. Stoddart, J.-P. Sauvage and O. M. Yaghi, *Angew. Chem. Int. Ed.*, 2012, **51**, 2160-2163.
148. Q. Li, W. Zhang, O. Š. Miljanić, C. B. Knobler, J. F. Stoddart and O. M. Yaghi, *Chem. Commun.*, 2010, **46**, 380-382.
149. Q. Li, C.-H. Sue, S. Basu, A. K. Shveyd, W. Zhang, G. Barin, L. Fang, A. A. Sarjeant, J. F. Stoddart and O. M. Yaghi, *Angew. Chem. Int. Ed.*, 2010, **49**, 6751-6755.
150. Q. Chen, J. Sun, P. Li, I. Hod, P. Z. Moghadam, Z. S. Kean, R. Q. Snurr, J. T. Hupp, O. K. Farha and J. F. Stoddart, *J. Am. Chem. Soc.*, 2016, **138**, 14242-14245.
151. M. Dresselhaus, G. Dresselhaus and R. Saito, *Carbon*, 1995, **33**, 883-891.
152. F. Li, H. M. Cheng, S. Bai, G. Su and M. S. Dresselhaus, *Appl. Phys. Lett.*, 2000, **77**, 3161-3163.
153. J. Hone, M. Whitney, C. Piskoti and A. Zettl, *Phys. Rev. B.*, 1999, **59**, R2514-R2516.
154. T. W. Odom, J.-L. Huang, P. Kim and C. M. Lieber, *Nature*, 1998, **391**, 62-64.
155. M. F. L. De Volder, S. H. Tawfik, R. H. Baughman and A. J. Hart, *Science*, 2013, **339**, 535-539.
156. M. Davenport, *Chem. Eng. News*, 2015, **93**, 10-15.
157. F. Yang, X. Wang, D. Zhang, J. Yang, D. Luo, Z. Xu, J. Wei, J.-Q. Wang, Z. Xu and F. Peng, *Nature*, 2014, **510**, 522.
158. H. An, A. Kumamoto, H. Takezaki, S. Ohyama, Y. Qian, T. Inoue, Y. Ikuhara, S. Chiashi, R. Xiang and S. Maruyama, *Nanoscale*, 2016, **8**, 14523-14529.
159. B. Aleman, M. M. Bernal, B. Mas, E. M. Pérez, V. Reguero, G. Xu, Y. Cui and J. J. Vilatela, *Nanoscale*, 2016, **8**, 4236-4244.
160. J. Liu, C. Wang, X. Tu, B. Liu, L. Chen, M. Zheng and C. Zhou, *Nat. Commun.*, 2012, **3**, 2205/2201-2205/2207.
161. M. C. Hersam, *Nat. Nanotechnol.*, 2008, **3**, 387.
162. X. Tu, S. Manohar, A. Jagota and M. Zheng, *Nature*, 2009, **460**, 250-253.
163. M. Zheng and E. D. Semke, *J. Am. Chem. Soc.*, 2007, **129**, 6084-6085.
164. G. Ao, C. Y. Khrpin and M. Zheng, *J. Am. Chem. Soc.*, 2014, **136**, 10383-10392.
165. Z. Hu, J. M. M. L. Comeras, H. Park, J. Tang, A. Afzali, G. S. Tulevski, J. B. Hannon, M. Liehr and S.-J. Han, *Nat. Nanotechnol.*, 2016, **11**, 559.
166. E. Burzurí, D. Granados and E. M. Pérez, *ACS Appl. Nano Mater.*, 2019, 1-19.
167. P. M. Ajayan and J. M. Tour, *Nature*, 2007, **447**, 1066.
168. P. Singh, S. Campidelli, S. Giordani, D. Bonifazi, A. Bianco and M. Prato, *Chem. Soc. Rev.*, 2009, **38**, 2214-2230.
169. M. A. Hamon, J. Chen, H. Hu, Y. Chen, M. E. Itkis, A. M. Rao, P. C. Eklund and R. C. Haddon, *Adv. Mater.*, 1999, **11**, 834-840.
170. M. Kanungo, H. Lu, G. G. Malliaras and G. B. Blanchet, *Science*, 2009, **323**, 234-237.
171. Y.-L. Zhao and J. F. Stoddart, *Acc. Chem. Res.*, 2009, **42**, 1161-1171.
172. N. Nakashima, Y. Tomonari and H. Murakami, *Chem. Lett.*, 2002, **31**, 638-639.
173. R. J. Chen, Y. Zhang, D. Wang and H. Dai, *J. Am. Chem. Soc.*, 2001, **123**, 3838-3839.
174. S. M. Bachilo, M. S. Strano, C. Kittrell, R. H. Hauge, R. E. Smalley and R. B. Weisman, *Science*, 2002, **298**, 2361-2366.
175. M. C. LeMieux, M. Roberts, S. Barman, Y. W. Jin, J. M. Kim and Z. Bao, *Science*, 2008, **321**, 101-104.
176. F. Wang, K. Matsuda, A. F. M. M. Rahman, X. Peng, T. Kimura and N. Komatsu, *J. Am. Chem. Soc.*, 2010, **132**, 10876-10881.
177. X. Peng, N. Komatsu, T. Kimura and A. Osuka, *J. Am. Chem. Soc.*, 2007, **129**, 15947-15953.



178. X. Peng, N. Komatsu, S. Bhattacharya, T. Shimawaki, S. Aonuma, T. Kimura and A. Osuka, *Nat. Nanotechnol.*, 2007, **2**, 361-365.
179. F. Diederich, C. Dietrich-Buchecker, J.-F. Nierengarten and J.-P. Sauvage, *J. Chem. Soc., Chem. Commun.*, 1995, 781-782.
180. N. Armaroli, F. Diederich, C. O. Dietrich-Buchecker, L. Flamigni, G. Marconi, J.-F. Nierengarten and J.-P. Sauvage, *Chem. Eur. J.*, 1998, **4**, 406-416.
181. A. Mateo-Alonso and M. Prato, *Tetrahedron*, 2006, **62**, 2003-2007.
182. A. Mateo-Alonso, G. Fioravanti, M. Marcaccio, F. Paolucci, D. C. Jagesar, A. M. Brouwer and M. Prato, *Org. Lett.*, 2006, **8**, 5173-5176.
183. T. Da Ros, D. M. Guldi, A. F. Morales, D. A. Leigh, M. Prato and R. Turco, *Org. Lett.*, 2003, **5**, 689-691.
184. Y. Xu, R. Kaur, B. Wang, M. B. Minameyer, S. Gsaenger, B. Meyer, T. Drewello, D. M. Guldi and M. von Delius, *J. Am. Chem. Soc.*, 2018, **140**, 13413-13420.
185. M. Barrejón, A. Mateo-Alonso and M. Prato, *Eur. J. Org. Chem.*, 2019, **0**, 1-13.
186. M. R. Diehl, D. W. Steuerman, H.-R. Tseng, S. A. Vignon, A. Star, P. C. Celestre, J. F. Stoddart and J. R. Heath, *ChemPhysChem*, 2003, **4**, 1335-1339.
187. A. Star, Y. Liu, K. Grant, L. Ridvan, J. F. Stoddart, D. W. Steuerman, M. R. Diehl, A. Boukai and J. R. Heath, *Macromolecules*, 2003, **36**, 553-560.
188. Although MINTs do not feature stoppers, we have only been able to separate macrocycles and SWNTs in MINTs by calcination of the macrocycles. This is most likely due to a combination of the extreme length of the SWNTs and the relatively large number of macrocycles per SWNTs, which prevent macrocycles from "falling off" the SWNT thread. Taking this into account, and the criteria described in the introduction, we believe that MINTs are better defined as rotaxanes (and MIMs) than as pseudorotaxanes.
189. E. M. Pérez, *Chem. Eur. J.*, 2017, **23**, 12681-12689.
190. J. Calbo, A. Lopez-Moreno, A. de Juan, J. Comer, E. Ortí and E. M. Pérez, *Chem. Eur. J.*, 2017, **23**, 12909-12916.
191. A. de Juan, A. Lopez-Moreno, J. Calbo, E. Ortí and E. M. Pérez, *Chem. Sci.*, 2015, **6**, 7008-7014.
192. A. de Juan, M. Mar Bernal and E. M. Pérez, *ChemPlusChem*, 2015, **80**, 1153-1157.
193. S. Leret, Y. Pouillon, S. Casado, C. Navio, A. Rubio and E. M. Pérez, *Chem. Sci.*, 2017, **8**, 1927-1935.
194. K. Miki, K. Saiki, T. Umeyama, J. Baek, T. Noda, H. Imahori, Y. Sato, K. Suenaga and K. Ohe, *Small*, 2018, **0**, 1800720.
195. R. Chamorro, L. de Juan-Fernandez, B. Nieto-Ortega, M. J. Mayoral, S. Casado, L. Ruiz-González, E. M. Pérez and D. González-Rodríguez, *Chem. Sci.*, 2018, **9**, 4176-4184.
196. M. Blanco, B. Nieto-Ortega, J. A. de M. Vera-Hidalgo, A. Lopez-Moreno, S. Casado, E. M. Pérez, L. R. González, J. M. González-Calbet and H. Sawada, *Nat. Commun.*, 2018, **9**, 1-7.
197. A. Ortiz-Acevedo, H. Xie, V. Zorbas, W. M. Sampson, A. B. Dalton, R. H. Baughman, R. K. Draper, I. H. Musselman and G. R. Dieckmann, *J. Am. Chem. Soc.*, 2005, **127**, 9512-9517.
198. S. Chichak Kelly, A. Star, M. V. P. Altoé and J. F. Stoddart, *Small*, 2005, **1**, 452-461.
199. I. Hijazi, T. Bourgeteau, R. Cornut, A. Morozan, A. Filoramo, J. Leroy, V. Derycke, B. Jousseme and S. Campidelli, *J. Am. Chem. Soc.*, 2014, **136**, 6348-6354.
200. A. Mann Florian, J. Horlebein, F. Meyer Nils, D. Meyer, F. Thomas and S. Kruss, *Chem. Eur. J.*, 2018, **24**, 12241-12245.
201. A. de Juan, Y. Pouillon, L. Ruiz-González, A. Torres-Pardo, S. Casado, N. Martin, A. Rubio and E. M. Pérez, *Angew. Chem., Int. Ed.*, 2014, **53**, 5394-5400.
202. A. Lopez-Moreno and E. M. Pérez, *Chem. Commun.*, 2015, **51**, 5421-5424.
203. L. de Juan-Fernandez, P. W. Munich, A. Puthiyedath, B. Nieto-Ortega, S. Casado, L. Ruiz-González, E. M. Pérez and D. M. Guldi, *Chem Sci*, 2018, **9**, 6779-6784.
204. A. de Juan and E. M. Pérez, unpublished results.
205. E. Martinez-Perinan, A. de Juan, Y. Pouillon, C. Schierl, V. Strauss, N. Martin, A. Rubio, D. M. Guldi, E. Lorenzo and E. M. Pérez, *Nanoscale*, 2016, **8**, 9254-9264.
206. J. N. Coleman, U. Khan, W. J. Blau and Y. K. Gun'ko, *Carbon*, 2006, **44**, 1624-1652.
207. A. López-Moreno, B. Nieto-Ortega, M. Moffa, A. de Juan, M. M. Bernal, J. P. Fernández-Blázquez, J. J. Vilatela, D. Pisignano and E. M. Pérez, *ACS Nano*, 2016, **10**, 8012-8018.
208. K. S. Chichak, S. J. Cantrill, A. R. Pease, S.-H. Chiu, G. W. V. Cave, J. L. Atwood and J. F. Stoddart, *Science*, 2004, **304**, 1308-1312.
209. J. J. Danon, A. Krüger, D. A. Leigh, J.-F. Lemonnier, A. J. Stephens, I. J. Vitorica-Yrezabal and S. L. Woltering, *Science*, 2017, **355**, 159-162.
210. B. Lewandowski, G. De Bo, J. W. Ward, M. Pappmeyer, S. Kuschel, M. J. Aldegunde, P. M. E. Gramlich, D. Heckmann, S. M. Goldup, D. M. D'Souza, A. E. Fernandes and D. A. Leigh, *Science*, 2013, **339**, 189-193.
211. G. De Bo, M. A. Y. Gall, S. Kuschel, J. De Winter, P. Gerbaux and D. A. Leigh, *Nat. Nanotechnol.*, 2018, **13**, 381-385.
212. J. Berna, D. A. Leigh, M. Lubomska, S. M. Mendoza, E. M. Pérez, P. Rudolf, G. Teobaldi and F. Zerbetto, *Nat. Mater.*, 2005, **4**, 704-710.
213. T. Ashirov and A. Coskun, *Chem*, 2018, **4**, 2260-2262.
214. M. Ikegame, K. Tajima and T. Aida, *Stud. Surf. Sci. Catal.*, 2003, **146**, 517-522.
215. S. Angelos, E. Johansson, J. F. Stoddart and J. I. Zink, *Adv. Funct. Mater.*, 2007, **17**, 2261-2271.
216. R. Klajn, L. Fang, A. Coskun, M. A. Olson, P. J. Wesson, J. F. Stoddart and B. A. Grzybowski, *J. Am. Chem. Soc.*, 2009, **131**, 4233-4235.
217. A. Coskun, P. J. Wesson, R. Klajn, A. Trabolsi, L. Fang, M. A. Olson, S. K. Dey, B. A. Grzybowski and J. F. Stoddart, *J. Am. Chem. Soc.*, 2010, **132**, 4310-4320.